Soft Matter

A Textile-Reinforced Composite Vascular Graft that Modulates Macrophage Polarization and Enhances Endothelial Cell Migration, Adhesion and Proliferation

Journal:	*Soft Matter*
Manuscript ID	SM-ART-09-2022-001190.R1
Article Type:	Paper
Date Submitted by the Author:	28-Dec-2022
Complete List of Authors:	Zhang, Fan; North Carolina State University, Wilson College of Textiles Tao, Hui; Donghua University, College of Textiles Gluck, Jessica; North Carolina State University, Wilson College of Textiles Wang, Lu; Donghua University College of Textiles, Daneshmand, Mani; Emory University School of Medicine, Department of Surgery King, Martin; North Carolina State University, Wilson College of Textiles

SCHOLARONE™
Manuscripts

A Textile-Reinforced Composite Vascular Graft that Modulates Macrophage Polarization and Enhances Endothelial Cell Migration, Adhesion and Proliferation *in vitro*

Fan Zhang[1,], Hui Tao[2], Jessica M. Gluck[1], Lu Wang[2], Mani A. Daneshmand[3], Martin W. King[1,2,*]*

[1]Wilson College of Textiles, North Carolina State University, Raleigh, NC 27606, USA
[2]College of Textiles, Donghua University, Shanghai, 201620, China
[3]Department of Surgery, School of Medicine, Emory University, Atlanta, Georgia 30322, USA
[*]E-mail: fzhang12@ncsu.edu, mwking2@ncsu.edu

Keywords: tissue-engineered vascular graft, composite, fiber, hydrogel, macrophage, endothelial cell.

Abstract

At the present time, there is no successful off-the-shelf small-caliber vascular graft (< 6 mm) for the repair or bypass of the coronary or carotid arteries. In this study, we engineer a textile-reinforced hydrogel vascular graft. The textile fibers are circularly knitted into a flexible yet robust conduit to serve as the backbone of the composite vascular graft and provide the primary mechanical support. It is embedded in the hydrogel matrix which seals the open structure of the knitted reinforcement and mediates cellular response toward a faster reendothelization. The mechanical properties of the composite vascular graft, including bursting strength, suture retention strength and radial compliance, significantly surpass the requirement for the vascular graft application and can be adjusted by altering the structure of the textile reinforcement. The addition of hydrogel matrix, on the other hand, improves the survival, adhesion and proliferation of endothelial cells *in vitro*. The composite vascular graft also enhances macrophage activation and upregulates M1 and M2 related gene expression, which further improves the endothelial cell migration that might favor the reendothelization of the vascular

graft. Taken together, the textile-reinforced hydrogel shows it potential to be a promising scaffold material to fabricate a tissue engineered vascular graft.

1. Introduction

Vascular diseases, such as coronary heart disease, cerebrovascular disease, and peripheral arterial disease, are among the leading causes of death [1]. They are typically caused by atherosclerosis induced narrowing or occlusion of blood vessels and cause ischemia of tissues and organs [2]. The current treatment of these diseases ranges from a lifestyle change, through prescription medicines to surgical interventions [3]. One of the surgical treatments is to use a vascular graft to replace or bypass the affected blood vessels. The current gold standard is to use an autologous vascular graft such as the patients' own saphenous vein or mammary artery. However, in the situation of systemic disease or secondary surgery, some patients do not have appropriate and healthy blood vessels that can be used. Although synthetic vascular grafts have long been commercialized and used for the replacement and bypass of large-caliber arteries, they are known to fail in small-caliber vessels (< 6 mm) due to acute thrombosis and graft stenosis [4].

Despite extensive efforts in the area, there is currently no small-diameter vascular graft available on the market for the bypass or replacement of a small caliber blood vessels, such as the coronary, carotid and peripheral arteries. To address this issue, tissue-engineered vascular grafts (TEVGs) have been proposed as a promising solution. They are designed to promote the regeneration of the vascular tissue and restoration of the vascular structure and function, so as to mimic the native blood vessel both mechanically and biologically.

In the design of TEVG scaffolds, one of the dilemmas is to achieve a balance between the mechanical properties and the biological performance. Synthetic degradable polymers, such as poly(lactic acid) (PLA), poly(glycolic acid) (PGA), polycaprolactone (PCL) or their

copolymers, have been widely researched and used in Class 3 medical devices because of their superior mechanical strength, biodegradability and low cytotoxicity [5,6]. However, they have also been implicated to elicit chronic inflammation that does not favor vascular regeneration [7]. On the contrary, natural polymer-hydrogels have been widely used in tissue engineering and regenerative medicine due to their bioactivity that rapidly resolves acute inflammation and promotes tissue cell ingrowth [8,9].Yet their application in load-bearing devices is limited because of their inferior mechanical strength.

Therefore, in this study, we designed a textile-reinforced hydrogel composite material in order to fabricate a scaffold for TEVG that combined the mechanically superior synthetic PLA fibers and bioactive gelatin methacryloyl (GelMA) hydrogel. The composite material harnesses the strong mechanical strength of PLA, the compliance of a knitting structure, as well as the bioactivity of GelMA hydrogel to modulate the inflammatory response and promote endothelization of the vascular graft.

PLA is a biodegradable polyester that has been broadly used in tissue engineering and medical implants [10]. It is hydrolyzed into lactic acid, which is a natural metabolic product of the human body which catabolizes into water and carbon dioxide. PLA has been used in Class 2 and Class 3 medical devices approved by the Food and Drug Administration [11]. In our previous study, PLA was also used as the supporting material to reinforce collagen threads for the fabrication of a TEVG [6,12]. The PLA fibers had sufficient mechanical strength to provide satisfactory mechanical properties to the vascular graft [6]. Using a circular knitting technique, we were able to fabricate a seamless tubular PLA/collagen conduit to serve as a vascular graft [6,13]. The knitting conduit was flexible and compliant, making it suitable for the vascular graft application [5,6,13].

Although textiles fabricated from PLA yarn have shown satisfactory mechanical robustness and radial compliance, they lack bioactivity, such as cell binding motifs to facilitate cell adhesion. It has also been reported that PLA prolongs the local inflammatory response, elicits a mild foreign body reaction, and retards tissue regeneration, especially in vascular applications [6,11,13].

GelMA hydrogel is a gelatin-based hydrogel that contains a significant water content and interconnecting pores. The high total porosity of the hydrogel supports nutrient transport, promotes cell penetration and allows microvasculature ingrowth [14]. Due to its gelatin backbone, the hydrogel can also provide cells with a soft surface and integrin binding sites that resemble the extracellular matrix (ECM) [8]. While retaining these beneficial features, gelatin is more accessible and less expensive compared to ECM proteins, making it an ideal raw material for tissue engineering applications. Methacrylation on its backbone allows crosslinking of the gelatin molecules into a hydrogel network while still maintaining its degradability by enzymes such as collagenase and matrix metallopeptidase 9 [9]. However, for load bearing applications such as a vascular graft, the GelMA hydrogel alone is not strong enough with regards to it mechanical properties. Given that, the combination of PLA and GelMA in this study leverages the mechanical robustness of PLA and the bioactivity of GelMA, we believe that the resultant vascular graft will be both mechanically strong and biologically active to facilitate vascular regeneration.

Endothelization is a critical step in the regeneration process of a TEVG. After implantation, rapid endothelium formation on the luminal surface of the TEVG can reduce coagulation and thrombus formation at the blood contacting surface and ensure patent functioning of the blood vessel [15]. Recent studies have uncovered that the macrophage plays a pivotal role in the endothelization of a TEVG. Macrophages are innate immune cells that are rapidly recruited to the surface of a biomaterial after implantation. They are a plastic cell type that can assume

different phenotypes and release distinct sets of cytokines and chemokines that regulate cellular activities [25]. Among their many subtypes, pro-inflammatory M1 macrophages are known to drive inflammation. The initial influx of macrophages and the acute inflammatory process can eliminate contaminants from the wound and initiate angiogenesis [16], which is beneficial to the endothelization of TEVG. However, a prolonged presence of M1 macrophages can cause adverse effects such as the formation of the fibrotic encapsulation around the graft material and even restenosis of the graft [17]. On the other hand, pro-regenerative M2 macrophages can mitigate inflammation, stabilize the vascular cells and facilitate the maturation of the blood vessel [40]. Therefore, in this *in vitro* study, we investigated the response of macrophages to our composite vascular graft and evaluated their impacts on endothelial cell activity.

In the present study, we fabricated a textile/hydrogel composite vascular graft so as to meet the requirements for both mechanical and biological performance. In order to determine the *in vitro* performance of our vascular graft, there were four objectives in this study: a) optimize the mechanical properties of the composite vascular graft; b) determine the cytocompatibility of the composite graft to macrophages and endothelial cells; c) measure the macrophage gene expression elicited by the composite vascular graft; and d) evaluate the effect of macrophages on endothelial cell activity.

2. Experimental

2.1 Fabrication of the composite vascular graft

2.1.1 Preparation of the textile reinforcement

The textile reinforcement was fabricated as described in [6,13]. Briefly, a 150 denier 92 filament PLA yarn was used (Xinxiang Sunshine Textiles Co Ltd., China). The molecular weight of the PLA was 140,909 ± 2,921 g/mol with a 1.57 ± 0.01 PDI. Two and 3 ends of the PLA yarn were plied at 100 turns/m of S twist on a DirecTwist® twisting machine (Agteks Ltd., Turkey) at a speed of 1000 turns/min (**Figure 2A**). These two plied PLA yarns and the singles

yarn were fed into a 16-needle circular knitting machine (**Figure S2A**) (Lamb Knitting Machine Corp., Chicopee, MA) to knit a 4 mm diameter tubular seamless textile conduit (**Figure 1B**). The edges of the textile conduit were cut with a hot cautery knife to heat-set the free ends and prevent the structure from unraveling.

2.1.2 Preparation of the hydrogel matrix

To fabricate the GelMA hydrogel matrix, gelatin from porcine skin was chemically modified using methacrylic anhydride (MAAH) as described by Loessner et al [9]. Briefly, 10% gelatin was fully dissolved in Dulbecco's phosphate-buffered saline (DPBS) (HyClone) at 50˚C and 0.8mL MAAH per gram of gelatin was added dropwise. The reaction was conducted in a water bath maintained at 50˚C for 2.5 h and was stopped by diluting the mixture 1:3 using DPBS at 40 ˚C. The mixture was centrifuged at 3500 g-force, and the supernatant was dialyzed against DI water for 1 week to remove unreacted MAAH. The dialyzed solution was lyophilized for 1 week and the powder was stored at -20˚C until use. The degree of modification of the GelMA was measured using nuclear magnetic resonance (NMR) and different batches showed similar levels of modification with an average value of 50% (**Figure S1**).

To make the precursor solution of the hydrogel, GelMA powder was dissolved in DPBS at a concentration of 10% w/v, followed by adding 2.5% final concentration of Irgacure 2959 (2-hydroxy-4’-(2-hydroxyethoxy)-2-methylpropiophenone). All the materials were purchased from Millipore Sigma unless specified.

2.1.3 Fabrication of the composite vascular graft

To prepare the composite vascular graft, the tubular knitted textile reinforcement was mounted on a Teflon rod (McMaster-Carr) and inserted in a custom designed and fabricated Teflon mold (McMaster-Carr) as shown in **Figure S2B**, and the GelMA precursor solution was infused into the mold. The whole structure was cooled to -20˚C for 10 min to physically crosslink the gel so as to maintain the shape of the structure. Then the mold was removed, and the composite

vascular graft was mounted on a rotating cylinder and crosslinked while rotating using ultraviolet light (UVP, Analytik Jena US) at a wavelength of 365 nm for 20 min. The resulting vascular grafts are shown in their hydrated state in **Figures S2C** and S**2D**. For storage, the grafts were frozen at -80˚C, lyophilized at -50˚C (Labconco lyophilizer) for 3-4 days and then stored at -20˚C until used. Lyophilized vascular grafts are shown in **Figures S2E and S2F**.

2.2 Structure analysis

To observe the morphology and quantify the pore size of the textile, hydrogel, and textile/hydrogel composite samples, scanning electron microscope (SEM) images were taken at 30× and 300× using a Phenom G1 desktop SEM (Thermo Fisher Scientific, USA). Samples containing hydrogel were freezed at -80˚C overnight and lyophilized at -50˚C over 3 days before imaging. All the samples were sputter-coated with a mixture of gold and platinum. The morphology of the textile reinforcement and hydrogel surface was observed using an inverted optical microscope (Axiovert 100A, Zeiss, Germany), which enabled the largest opening at the surface of the specimen to be measured by ImageJ software. Three images were taken of each specimen, and 3 specimens were included for each sample. The average pore size and pore size distribution were calculated and are reported in **Figure 1**.

2.3 Hematoxylin and eosin staining

To observe the cross-section of the structure of the hydrated composite vascular grafts and to distinguish the knitted textile yarns from the hydrogel, the composite grafts were fixed in 3% formaldehyde for 24 h, followed by serial dehydration in 70%, 95% and 100% ethanol (KOPTEC) and SafeClear™ II for 45 min in each reagent. The samples were then embedded in Paraplast Plus embedding medium (Leica) and sectioned to a thickness of 10 μm on a microtome (Microm HM 315, Thermo Fisher, USA). The sections were stained by hematoxylin and eosin and observed under a brightfield optical microscope (EVOS FL Auto 2 microscope, Thermo Fisher, USA) at 4x magnification. Individual images were combined to show the entire

cross-section of the graft. All the materials were purchased from Fisher Scientific unless specified.

2.4 Water permeability test

Water permeability is a key feature to estimate the blood permeability of a vascular graft and has been used to determine if a vascular graft needs pre-clotting before implantation [19]. In general, a graft with a water permeability greater than 300 mL/cm^2/min needs to be pre-clotted to prevent hemorrhage after implantation [19]. In this study, the composite vascular graft was immersed in 1X PBS overnight to equilibrate the hydrogel. A hydrated graft measuring 5 cm long (L) with a diameter of 4.5 mm (D) was mounted between 2 nozzles to form a closed circuit for water to pass through under controlled pressure. Water permeability was determined by measuring the volume (Q) of deionized water that leaked through the vascular graft wall under an intraluminal water pressure of 13.5 kPa (100 mmHg) for 10 minutes (t). Water permeability (W) was calculated using **Equation 1**.

$$\mathrm{W} = \frac{\mathrm{Q}}{(\mathrm{L} \times \pi\mathrm{D}) \times \mathrm{t}} \quad (1)$$

2.5 Degradation assay

The degradation of the three samples was monitored *in vitro* for 3 weeks. The freshly made materials were freeze dried and weighed (W_0) and then immersed in 2 unit/mL collagenase I (Gibco) solution at 37 ˚C. The collagenase I solution was replaced every week. At each timepoint the samples were washed in deionized water 3 times and immersed overnight before lyophilizing. The lyophilized samples were weighed (*Wt*) and the remaining weight (*Wr*) was calculated using **Equation 2**.

$$W_r(\%) = \frac{W_0 - W_t}{W_0} \times 100 \quad (2)$$

2.6 Mechanical tests

2.6.1 Probe bursting test

A probe bursting test was used to measure the bursting strength of the vascular graft prototype samples as described previously [6]. Briefly, a 1cm long tubular sample was immersed in PBS overnight to rehydrate. It was then cut open in the longitudinal direction, flattened and mounted between the 2 plates with a 4mm diameter pin hole in the center to allow a 2mm diameter probe (R = 1mm) to pass through. The probe was connected to the crosshead of an MTS mechanical tester with a 50N load cell and a crosshead speed of 1 mm s^{-1}. Three replicates were measured for each sample. The bursting stress (MPa) was calculated by dividing the maximum bursting load (N) by the surface area of the spherical probe ($2\pi R^2$).

2.6.2 Suture retention test

The suture retention test was performed on an MTS mechanical tester using a 50N load cell. Samples were rehydrated by immersing in PBS overnight. The bottom end of each specimen was mounted between pneumatic clamps while a 3–0 braided nylon suture was passed through the top of the specimen 2 mm away from the upper cut edge. Both ends of the suture were fixed to a capstone clamp connected to the crosshead on a MTS mechanical tester which moved with a speed of 1 mm s^{-1}. Three replicates were tested for each sample. The average maximum force (N) was reported.

2.6.3 Radial dynamic compliance

Radial dynamic compliance of the vascular graft samples was measured using an Electroforce® Biodynamic Mechanical Test System Model 5175 (TA Instruments, New Castle, DE, USA). The test was performed following the standard ISO 7198: 2016 test method. A 5-cm-long conduit sample was immersed in PBS to rehydrate overnight and was then mounted on the tester with a 4.5mm diameter highly deformable polyurethane tube inserted inside so as to transfer the intraluminal water pressure wave to the wall of the vascular graft. The water flow rate was 100 mL/min, and a pulsatile frequency was set at 1 Hz. The external diameter changes were monitored and measured by a laser micrometer in response to 3 different dynamic pressure

loading regimes, namely 50–90 mmHg, 80–120 mmHg and 110–150 mmHg, mimicking the hypotensive, normotensive and hypertensive human blood pressure conditions. Each sample was run for 20 cycles between each pressure loading regime. The radial compliance (%/100 mmHg) was calculated according to the **Equation 3**.

$$\%\ Compliance = \frac{R_{p_s} - R_{p_d}}{R_{p_d} \times (p_s - p_d)} \times 10^4 \quad (3)$$

where,

R_p = the pressurized internal radius, in mm.

p_d = the diastolic pressure in mmHg.

p_s = the systolic pressure in mmHg.

2.7 THP-1 cell culture

The human leukemia monocytic cell line THP-1 cells (TIB-202™, ATCC), were cultured in high-glucose RPMI 1640 media (ATCC) supplemented by 10% fetal bovine serum (Atlas Biologicals) and 1% penicillin streptomycin antibiotic reagent (Gibco). The cells were seeded at a concentration of 4×10^5 cells/mL. The cell culture media was added to the cell suspension every 2-3 days to keep the cell concentration below 1×10^6 cells/mL all the time. A complete media change was performed every week by centrifuging the cells at 200 g force for 10 min. The cells were expanded up to passage 7 before use.

Before seeding the THP-1 cells on the scaffold materials, the cells were activated into macrophages by treating cells with 200 ng/mL phorbol 12-myristate 13-acetate (PMA) (Sigma) for 24 h. After treatment, the cells become adherent and stopped proliferating. The cells were then washed in PBS and maintained in fresh cell culture media for at least 24 h. To lift cells from the surface, cells were incubated with Accutase® enzyme cell detachment medium (Invitrogen) for 10 min at 37 ˚C. The cells were seeded to the scaffolds at a density of 2.5×10^5 cells/cm^2 and the media was changed every other day.

An M1 control was induced by adding 100 ng/mL lipopolysaccharide (LPS) (Invitrogen) and an M2 control was induced by adding 40 ng/mL recombinant human interleukin-4 (IL-4) (Peprotech).

2.8 Human umbilical vein endothelial cell culture

Human umbilical vein endothelial cells (HUVECs) (PCS-100-010™, ATCC) were expanded in vascular cell basal medium supplemented with endothelial cell growth kit-VEGF (ATCC). Cells were seeded on the scaffold material at a density of 2.5×10^5 cells/cm^2 unless otherwise specified. The cell culture media was changed every 3 days.

2.9 Live/Dead viability assay

The viability of the cells was measured using a LIVE/DEAD® cell imaging kit (Invitrogen) per manufacture's instruction. Live cells were imaged at an excitation/emission wavelength of 488/515 nm and dead cells at 570/602 nm using an EVOS FL Auto 2 imaging system (Thermo Fisher Scientific, USA) with an excitation/emission wavelength of 488/515 nm for live cells stained by calcein acetoxymethyl ester (calcein AM) and 570/602 nm for the nuclei of dead cells. Triplicate specimens were included for each sample material and at least 3 images were taken from each specimen. The number of live and dead cells were counted using ImageJ, and cell viability was calculated using **Equation 4**.

$$Cell\ viability\ (\%) = \frac{\#of\ live\ cells}{\#of\ live\ cells + \#of\ dead\ cells} \times 100 \quad (4)$$

2.10 Immunofluorescence staining and imaging

The macrophage morphology was analyzed by staining the filament actin (F-actin) using Alexa Fluor™ 488 Phalloidin (Invitrogen). The samples were fixed in 4% paraformaldehyde (Fisher) for 20 min and permeabilized using TritonX-100 (Fisher) for 30 min. Then the samples were blocked for 1 h using 2% bovine serum albumin (Fisher) and 2% goat serum (Gibco) in 1% Tween 20 (Fisher) in DPBS (Gibco), followed by incubating with the Alexa Fluor™ 488

Phalloidin (1:200 in blocking buffer) at 4˚C overnight. The samples were then counterstained by Hoechst 33342 (Invitrogen) at 4˚C overnight followed by the addition of ProLong™ Gold antifade reagent (Invitrogen). Between these steps, copious washes were undertaken using 1% Tween 20 in DPBS. The stained samples were imaged using a Laser Scanning Confocal Microscope (LSM880, Zeiss, Germany). Triplicate specimens were included for each sample type, and at least 3 images were taken from each sample.

2.11 Gene expression analysis

The total RNA was extracted from the cell seeded samples using the total RNA purification plus micro kit (Norgen Bioteck Corp) as per the manufacture's instructions. The concentration and purity of the extracted RNA was measured using a Nanodrop spectrometer (Thermo Fisher Scientific, USA). The RNA was converted to complementary DNA (cDNA) using a high-capacity cDNA reverse transcription kit (Applied Biosystems) in a MiniAmp Thermal Cycler (Applied Biosystems) as per the manufacture's instructions. A series of primers (Integrated DNA Technologies, Inc.) listed in **Table 1** were used to analyze the expression of specific genes. The cDNA was mixed with a specific primer and PowerTrack™ SYBR Green Master Mix (Applied Biosystems) and amplified in a QuantStudio 3 real-time PCR system (Applied Biosystems, Thermo Fisher Scientific) for qPCR analysis. Triplicate specimens were included for each type of sample material and for each reaction. The gene expressions were analyzed by the $2^{-\Delta\Delta Ct}$ method. All gene expressions were normalized to the endogenous control gene glyceraldehyde-3-phosphate dehydrogenase (GAPDH) and the tissue culture plate (TCP) control. When the power change was greater than 2, it was considered an upregulation, and when it was smaller than 0.5, it was considered as a downregulation.

Table 1. PCR primers

Gene	Function	Forward	Reverse
IRF5	M1 inducing transcription factor	CCAGCCAGGACGGAGATAAC	CATCCACGCCTTCGGTGTAT
TNF-α	TNF-α promotes leukocytes recruitment in the early state of atherosclerosis. Knockout of TNF-α or administration of agents that reduce TNF-α activity were both found to	CTGCTGCACTTTGGAGTGAT	AGATGATCTGACTGCCTGGG

	reduce atherosclerosis and endothelial adhesion.		
IL-1β	IL-1β was implicated to promote coagulation, leukocyte-to-EC adhesion, and SMC proliferation.	ATGATGGCTTATTACAGTGGCAA	GTCGGAGATTCGTAGCTGGA
STAT6	M2 inducing transcription factor	ATGGGGCAACAGAAAAGATG	GCACAGAAGACAGCAGCAAG
IL-10	IL-10 was found to increase the EPC survival, migration, and VEGF expression in the MI murine model. It is also inhibitor of TNF-a, IFN-c, IL-1b.	TCAAGGCGCATGTGAACTCC	GATGTCAAACTCACTCATGGCT
CD206	M2 marker	AAGGCGGTGACCTCACAAG	AAAGTCCAATTCCTCGATGGTG
VEGF	VEGF promotes endothelial proliferation, migration, and sprouting of tip cells in the early stages of angiogenesis	AGGGCAGAATCATCACGAAGT	AGGGTCTCGATTGGATGGCA
PDGF	Myeloid cell-derived PDGF-B contribute to the reduced neotissue formation and retarded polymer degradation of vascular graft in vivo. PDGF-BB KO in a murine model caused macrophage apoptosis and reduced the macrophage population in the TEVG.	CTCGATCCGCTCCTTTGATGA	CGTTGGTGCGGTCTATGAG
TGFβ1	TGF-β increases vascular smooth muscle cell proliferation through the Smad3 and ERK MAPK pathways. It was also implicated to enhance intimal hyperplasia. Downregulation of inflammatory cytokine in monocytes and macrophages; MMP9-dependent activation.	CAATTCCTGGCGATACCTCAG	GCACAACTCCGGTGACATCAA
TIMP3	TIMP3 mediate vascular stenosis and remodeling.	ACCGAGGCTTCACCAAGATG	CATCATAGACGCGACCTGTCA
GAPDH	Endogenous control	AAGGTGAAGGTCGGAGTCAAC	GGGGTCATTGATGGCAACAATA

2.12 Conditioned media collection and treatment

In order to study how macrophages cultured on the scaffold materials would influence HUVEC activity, the supernatant conditioned media (CM) from the THP-1 cells cultured on the material samples were collected every other day. The media were filtered through a 0.2 μm polyethersulfone (PES) membrane to remove cellular debris and were then stored at -20˚C until use.

HUVECs were seeded at a density of 1 x 10^4 cells/well on 24-well plates. The conditioned media were added to the HUVECs together with the complete HUVEC culture media at a ratio of 1:1. A media control was included with RPMI basal media and complete HUVEC culture media at a ratio of 1:1 to eliminate the role of HUVEC media on EC migration.. The media were replenished every 3 days. The metabolic activity of HUVECs was measured at 1, 4 and 7 days after cell seeding and the cell number was quantified to analyze the HUVEC proliferation over 7 days under the CM treatment.

2.13 HUVEC metabolic activity and proliferation assay

The alamarBlue® assay (Invitrogen) was used to measure the cell metabolic activity by following the manufacture's instructions. Briefly, cells were incubated for 2 hours at 37 °C in fresh cell culture media supplemented with 10% (v/v) alamarBlue® reagent. Then, 100 μL reagent was added to a 96-well plate for fluorescence reading. The fluorescence was read at the excitation and emission frequencies of 550 nm and 590 nm respectively and any reduction in alamarBlue® reagent (% reduction) was calculated by **Equation 5**. The culture media plus 10% alamarBlue® reagent added to a blank well was used as the negative control. The positive control was prepared by autoclaving the media containing 10% alamarBlue® reagent for 15 min at 121 °C.

$$\%\ \text{Reduction} = \frac{\text{Exp.} - \text{Neg. ctrl}}{\text{Pos. ctrl} - \text{Neg. ctrl}} \times 100 \quad (5)$$

where,

Exp. = reading from the experimental sample.

Neg. ctrl. = reading from the negative control.

Pos. ctrl. = reading from the 100% positive control.

To quantify cell proliferation, a standard calibration curve has to be created recording the percentage reduction at different cell numbers from 5,000 to 40,000. The number of living cells on the scaffold was then calculated by comparing the percent reduction of cells on the samples to the calibration curve.

2.14 HUVEC migration

Human umbilical vein endothelial cells (HUVECs) were seeded at a density of 1.2×10^5 cells per well in a 48-well plate and incubated overnight. Using a 1000μL micropipette tip, the endothelial cells were scratched to create a straight wound as shown in **Figure 7**. The scratched

cells were washed off using 0.01M PBS. The conditioned media (CM) of the macrophages cultured with the different samples was mixed with endothelial cell media at a ratio of 1:1 and then added to the HUVECs. After a 24-hr treatment, 5μg/mL calcein acetoxymethyl ester (calcein AM) (Cayman Chemical) was added to stain the cytoplasm of the endothelial cells, and Hoechst (Invitrogen) was added to stain the cell nuclei. Microscopic images were taken using an EVOS FL Auto 2 imaging system (Thermo Fisher Scientific) with an excitation/emission wavelength of 488/515 nm for calcein AM and 357/447 nm for Hoechst. The relative wound area was calculated using **Equation 6**. A smaller wound area indicates faster cell migration.

$$Wound\ Area = \frac{A_0 - A_t}{A_0} \times 100 \quad (6)$$

where:

A_t is the wound area after 24 h of incubation.

A_0 is the initial wound area.

2.15 Statistics

Statistical analysis was performed using JMP Pro 15 software (SAS Institute). Means and standard deviations were calculated and are presented in Section 3. One-way analysis of variance and all-paired Tukey's post hoc test were used to identify statistical significances ($p<0.05$). Median was reported and non-parametricSteel-Dwass test was conducted when the data show a skewed distribution.

3. Results

3.1. Fabrication of the fiber-reinforced hydrogel vascular graft

In order to build a vascular graft that has sufficient mechanical robustness to maintain dimensional stability and normal healthy function as well as promote vascular tissue regeneration, we designed a textile fiber-reinforced hydrogel composite vascular graft (**Figure**

1A). A knitted 2-ply PLA conduit (**Figure 1B**) was fabricated from PLA multifilament yarns using a circular knitting machine (**Figure S2A**). This textile conduit served as the backbone and reinforcement of the composite vascular graft to provide primary mechanical support. It was inserted in a customized Teflon® mold (**Figure S2B**), and the GelMA hydrogel pre-polymer solution was infused into the mold and photo-crosslinked into the composite graft (**Figure 1C, Figures S2C-S2F**). **Figure 1D** shows a cross-sectional view of the composite graft stained with hematoxylin and eosin (H&E). The purple staining indicates GelMA hydrogel while the unstained pale material indicates PLA fibers. It can be observed from **Figure 1D** that PLA fibers were surrounded by the GelMA hydrogel, which can also be appreciated from the scanning electron microscopy (SEM) image in **Figure 1E**. **Figures 1E and 1F** show the surface of the composite at low and high magnifications respectively. In **Figure 1F**, it can be seen from the external surface of the composite graft that the PLA fibers were well embedded in the hydrogel matrix. The structure of the PLA textile is shown in **Figure 1G** (low magnification) and **Figure 1H** (high magnification), and the surface morphology of the hydrogel matrix is presented in **Figures 1I and 1J** (both at high magnification).

The SEM images also allow the measurement of the pore size area and distribution on the surface of the graft. It is noticeable that the knitted textile structure has large pores (**Figure 1L**), which can cause blood leakage through the vessel wall under internal pressure and require additional pre-clotting procedure before clinical use. After infusing the hydrogel matrix, these large pores on textiles were filled in by the GelMA hydrogel. As a result, the water permeability of the graft was reduced to a negligible level, ~ 5.5 $\mu L\ cm^{-2}\ min^{-1}$, which is critical to the normal clinical function of a vascular graft to prevent blood leakage through the porous knitted structure and regulate hemostasis.

The degradation profile of the three samples was investigated by immersing the materials in collagenase I solution over a period of 3 weeks (**Figure S3**). The PLA textile was relatively

stable with 96.9% weight remaining after 3 weeks. This allowed the composite graft to have a stable backbone to withstand applied mechanical forces and tensions. The GelMA hydrogel degraded faster and gradually lost 43.3% of its original weight over 3 weeks. This indicates that 56.7% of its original weight remained. Despite changes in mass, it was noted that the volume of the three samples did not change significantly. The gradual degradation of the GelMA matrix could potentially help cell infiltration and ECM deposition.

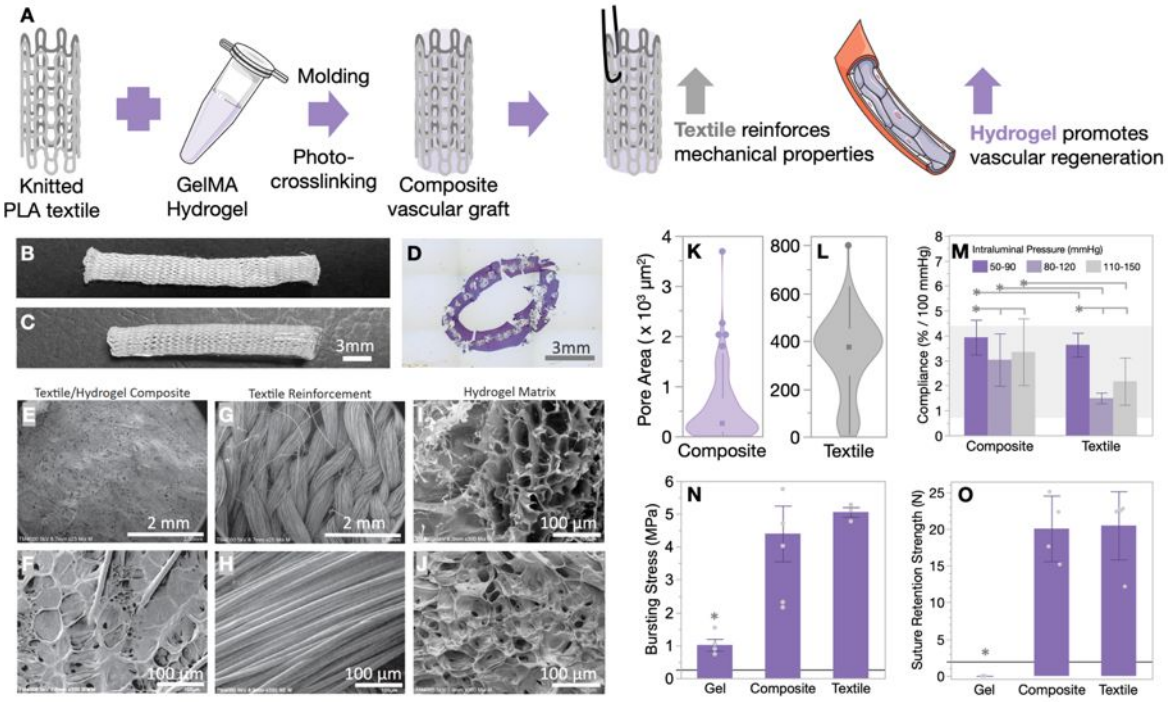

Figure 1. (A) Scheme of the experimental design and fabrication process for the composite vascular graft. (B) Gross photograph of the PLA textile and (C) the PLA/GelMA composite vascular graft. Scale bar = 3 mm. (D) H&E histological image of the cross section of the composite vascular graft. GelMA hydrogel matrix was stained in purple; PLA textile remained unstained in gray. Scale bar = 3 mm. (E-J) SEM images of (E-F) composite vascular graft compared to (G-H) 2-ply textile sample and (I-J) hydrogel matrix. Scale bar: (E & G) 2 mm, (F, H-J) 100 µm. (K-L) Pore size distribution of (K) composite vascular graft and (L) textile reinforcement. (M) Radial dynamic compliance of the textile and composite vascular grafts. Grey area on the background marked out the compliance range of a human saphenous vein graft [13, 18] (N) Bursting strength and (O) suture retention strength results for the three samples: the composite vascular graft, the hydrogel matrix and the textile reinforcement. The black lines indicate the minimum requirements for the vascular graft application [13, 18]. n=3. *$p<0.05$.

3.2 The composite vascular graft has sufficient mechanical strength

As required by the ISO 7198:2016 standard, *Cardiovascular implants and extracorporeal systems - Vascular prostheses, tubular vascular grafts, vascular patches*, a vascular graft must show sufficient mechanical strength for its safe use [20].

Radial dynamic compliance measures and predicts the ability of the graft wall to dilate and contract in response to intraluminal blood pressure. It is critical for the long-term patency of any vascular graft given that numerous studies have reported about complications and lost graft patency results from a mechanical mismatch between the graft and its adjoining natural vessel [18,21,22]. In the normal human blood pressure range, the compliance of the composite vascular graft was 3.03 ± 0.69 %/100mmHg. At hypotensive and hypertensive blood pressure ranges, the compliance of the composite graft was 3.93 ± 1.05%/100mmHg and 3.35 ± 1.33 %/100mmHg respectively (**Table 2**). Although not completely matching the compliance of a human artery (5.9 ± 0.5 %/100mmHg [18]), the composite conduit showed compatible compliance to the reported compliance of a human saphenous vein graft (0.7-4.4%/100mmHg [13,18]), which is the current gold standard graft for bypass surgery. It also surpassed the compliance of traditional ePTFE (1.6 ± 0.2 %/100mmHg) and Dacron vascular grafts (1.9 ± 0.3 %/100mmHg) [18].

Table 2. Compliance results for the vascular graft samples

	Intraluminal Pressure (mmHg)	Textile reinforcement	Textile/hydrogel composite graft
Radial dynamic compliance (%/100mmHg)	50 - 90	3.63± 0.48	3.93 ± 0.69
	80 - 120	1.49 ± 0.22	3.03 ± 1.05
	110 – 150	2.17 ± 0.95	3.35 ± 1.33

Surprisingly, the composite vascular graft showed slightly improved compliance compared to the textile reinforcement under normotensive and hypertensive blood pressure ranges ($p<0.001$) (**Figure 1M** and **Table 2)**. Although the textile reinforcement had a better dilation response to the increase of intraluminal pressure compared to the composite, its ability to recover was not as good as for the composite graft. Adding the elastic hydrogel matrix contributed to the increase of the radial compliance of the composite graft. However, the hydrogel matrix sample

without textile reinforcement was mechanically too weak to survive the compliance test, and therefore no data was obtained.

Bursting strength is another important mechanical property because it indicates the amount of stress or internal pressure that the vascular graft can withstand prior to rupture. Due to the incorporation of the textile reinforcement, the bursting strength of the composite vascular graft (4.4 ± 2.1 MPa) was significantly improved compared to the hydrogel matrix sample (1.0 ± 0.4 MPa) ($p=0.0138$). All three samples exceeded the minimum requirement of 0.26 MPa bursting strength for a vascular graft (**Figure 1N**) [13].

Suture retention strength is critical to secure the anastomosis between a vascular graft and the adjoining native blood vessel. Inadequate suture retention strength can lead to fraying at the cut edge of the vascular graft which can cause dehiscence, suture line failure, bleeding and/or the formation of a false aneurysm. The hydrogel sample had insufficient suture retention strength, making it impossible to suture. Reinforced by the knitted textile component, the composite vascular graft showed a significantly improved suture retention strength of 20.06 ± 4.47 N, which far surpassed the minimum required suture retention strength of 2N (**Figure 3B**) [13].

3.3 The mechanical properties of the composite vascular graft were optimized by modifying the textile structure

Given that the textile reinforcement provided the mechanical strength to the composite vascular graft (**Figure 1)**, we were able to optimize the structure of the textile reinforcement by changing the number of PLA yarns that were plied together (**Figure 2A**). We then evaluated the impact of the number of plied yarns on the structure (**Figure 2E-H**) and the critical mechanical properties of the vascular graft, namely, the radial dynamic compliance (**Figure 2B**), the bursting strength (**Figure 2C**) and the suture retention strength (**Figure 2D**).

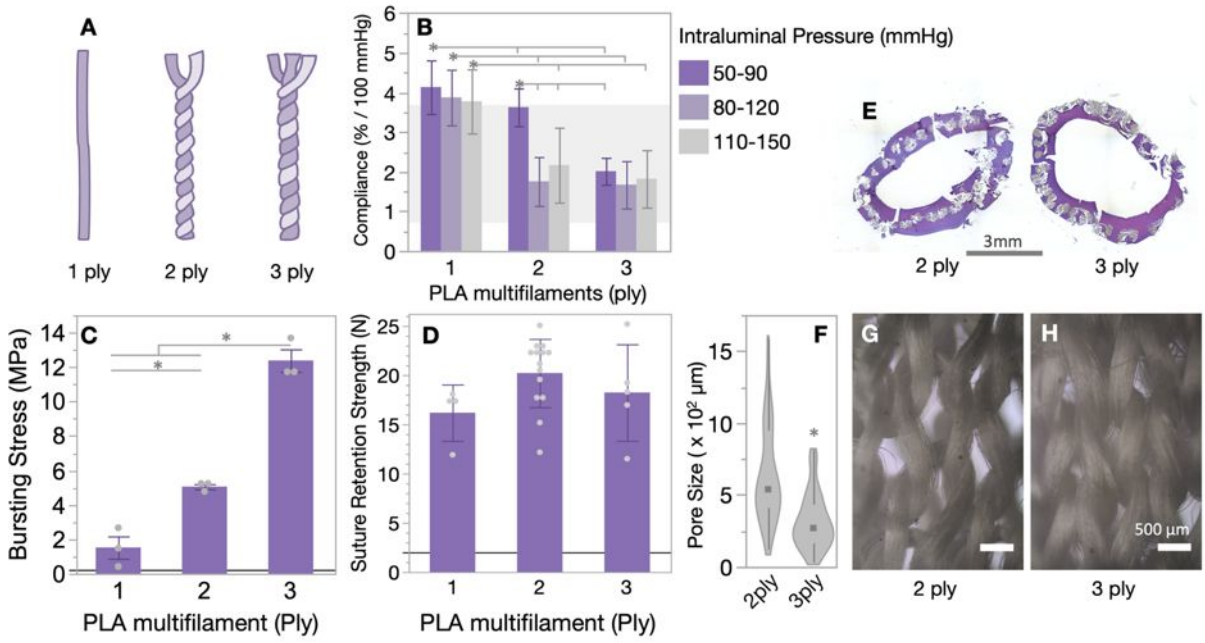

Figure 2. Optimization of the textile reinforcement. (A) Illustration of the structure of the PLA yarns used to fabricate the textile reinforcement. (B) Radial dynamic compliance of the tubular textile structure knitted from 1, 2 or 3 plies of PLA yarn under hypotensive (50-90mmHg), normotensive (80-120 mmHg) and hypertensive (110-150 mmHg) intraluminal pressure. Grey area on the background marked out the compliance range of a human saphenous vein graft obtained from the literature. (C) Bursting strength and (D) suture retention strength of the textile structure knitted from 1, 2 or 3 plies of PLA yarn. The black lines indicate the minimum requirements for a vascular graft. (E) H&E histological image of the composite vascular graft knitted from 2-ply (left) and 3-ply (right) PLA textile yarn. Scale Bar = 3 mm. (F) Pore size distribution of the 2-ply and 3-ply knitted textile structure. (G & H) Optical microscopic images of the structure knitted from (G) 2-ply and (H) 3-ply PLA yarn. Scale Bars= 500 µm. $n \geq 3$; *$p<0.05$.

One, two or three ends of PLA yarn were plied and fed into a circular knitting machine to knit a tubular textile structure (**Figure 2A**). The sample knitted from 1-ply PLA yarn was excessively loose and lacked structural stability, while those samples knitted from 2-ply and 3-ply yarns were more stable. Optical images of the 2-ply (**Figure 2G**) and the 3-ply structures (**Figure 2H**) showed that the 2-ply sample had larger pores (**Figure 2F**) and fewer fibers, which meant that the structure was looser than the 3-ply sample. It can also be observed from the cross-sectional views of the 2-ply and 3-ply composite grafts (**Figure 2E)** that there were fewer fibers in the 2-ply vascular graft sample compared to the 3-ply sample.

The 1-ply or singles knitted structure gave significantly larger compliance vales at different intraluminal pressures compared to the 2-ply and 3-ply samples. The 2-ply knitted structure also had a higher compliance compared to the 3-ply sample in the hypotensive blood pressure range, but similar compliances when operating within the normotensive and hypertensive ranges (**Figure 2B**). Such a decrease in the radial compliance of the 2-ply and 3-ply samples might be ascribed to a tighter knitted structure which increased the friction between fibers and reduced the inter-fiber spacing.

On the other hand, increasing the number of plies resulted in a stronger bursting strength (**Figure 2C**). It has been reported previously that increasing the tightness of the textile structure can improve the bursting strength of the fabric [6].

With the addition of the textile reinforcement, there was no significant improvement in the suture retention strength (**Figure 2D).** Yet all three samples showed a bursting strength and a suture retention strength that exceeded the minimum requirement for a vascular graft, as denoted by the black lines in **Figures 2C** and **2D**.

So when taking all the results into consideration, the 2-ply PLA knitted structure was selected as the optimum reinforcement for the composite vascular graft. Overall, the 1-ply or singles knitted structure showed good compliance and acceptable bursting and suture retention strength. However, its loose and easily deformable structure, makes it difficult to handle in a clinical setting. And while the strength of the 3-ply sample was high, its compliance was unacceptably low. Therefore, the 2-ply knitted structure was selected for further study of the composite vascular graft because of its relatively good compliance and superior strength and robustness.

3.4 Endothelial cell viability, adhesion and proliferation on the composite vascular graft

To determine if the material would favor endothelial cell survival and proliferation, HUVECs were seeded on the textile (**Figure 3A**), hydrogel (**Figure 3B**) and textile/hydrogel composite graft (**Figure 3C**) to evaluate the cytocompatibility of the material to HUVECs. Cells seeded on the tissue culture plate (TCP) were used as a control.

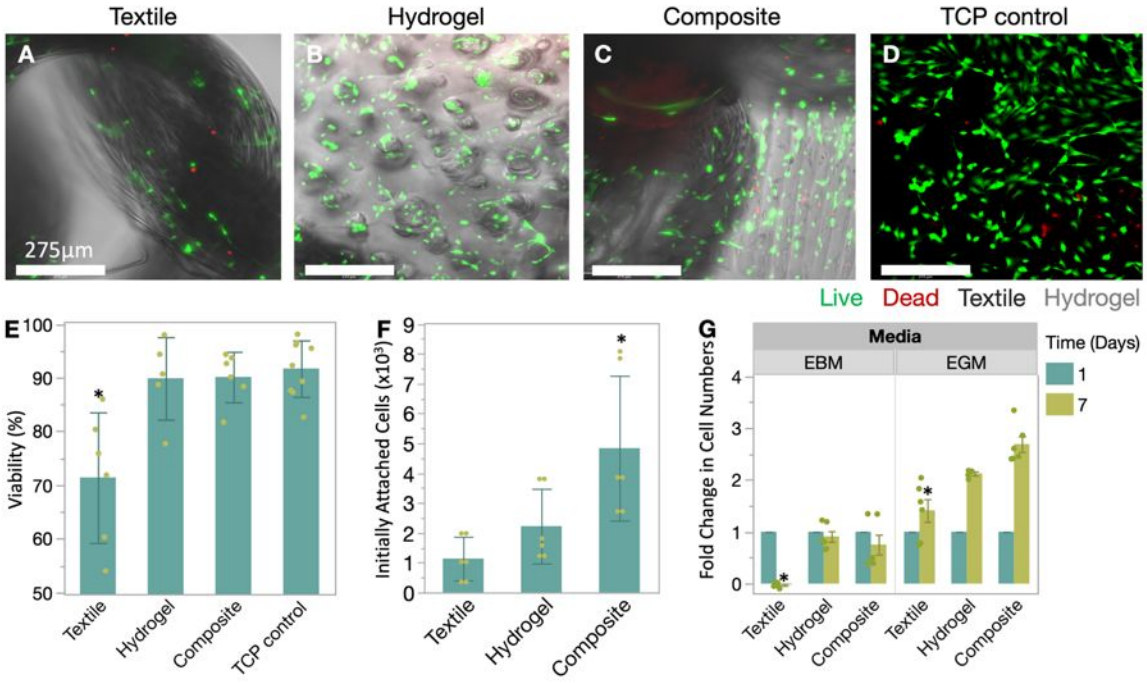

Figure 3. Endothelial cell growth on experimental samples *in vitro*. (A - D) Live/dead staining of cells cultured for one day on (A) PLA textile sample, (B) GelMA hydrogel, (C) textile/hydrogel composite sample and (D) tissue culture plate (TCP) as the control. Green = live cells, red = dead cells, black = textile, gray=hydrogel. Scale bar = 275 µm. (E) Cell viability of HUVECs after 3 days of *in vitro* culture. (F) Cells attached to scaffold after one day of *in vitro* cell culture. (G) Cell proliferation over 7 days of *in vitro* cell culture. Cell numbers were normalized to viable cells on each scaffold on Day 1. n=6, *p<0.05.

HUVECs exhibited significantly lower viability on the PLA knitted textile sample (71.4 ± 12.1 %) compared to the hydrogel sample (89.9 ± 7.7 %, p=0.0035), the composite sample (90.1 ± 4.7 %, p=0.0019) and the TCP control (91.7 ± 5.3 %, p=0.0003) (**Figure 3E)**. This demonstrates the important role of the hydrogel in improving HUVEC viability. Not only was the cell viability enhanced, but also the cell attachment was improved due to the addition of the hydrogel matrix. There was only a limited number of HUVECs (1140 ± 731) attached to the PLA textile sample one day after cell seeding, which may be due to the high porosity and/or

the lack of bioactivity (**Figures 3A & 3F**). While there appeared to be more cells attached to the hydrogel matrix (hydrogel (2226 ± 1251) compared to the textile sample (1140 ± 731), the difference was not significant (p= 0.4979) (**Figure 3B & 3F**). However, the composite scaffold showed a significantly higher number of attached cells (4838 ± 2425) one day after cell seeding (composite vs. textile: p=0.0036; composite vs. hydrogel: p=0.0357) (**Figures 3C & 3F**). The hydrogel matrix provided a more bioactive surface for cell attachment. So the addition of the hydrogel not only increased the surface area for cells attachment, but the combination of both the textile reinforcement and the hydrogel matrix also contributed to the improvement in HUVEC binding to the composite scaffold.

Cell metabolic activity remained high in the composite and hydrogel scaffolds when cultured in endothelial basal media (EBM) without the addition of serum and growth factors (**Figure 3G**). On the other hand, cells cultured on the textile scaffold under the same conditions showed only minimal metabolic activity (composite vs. textile: $p<0.0001$; composite vs. hydrogel: p=0.0118; hydrogel vs. textile: p=0.0002). The number of live cells was calculated by extrapolating a standard calibration curve with a series of known cell numbers. For example, the cell number on Day 7 was normalized to the cells attached to the scaffold on Day 1 to calculate the fold change, assuming the cell metabolic rate was the same. On Day 7, there was no viable cells on the textile scaffold in EBM. On the contrary, 91.0 ± 25.0 % cells seeded on the hydrogel scaffold remained alive in EBM, and 75.3 ± 46.9% cells remained on the composite scaffold. This comparison points to the fact that there were significant benefits in using the hydrogel matrix so as to maintain cell viability for up to 7 days *in vitro* even without the addition of serum and growth factors.

When serum and growth factors (EGM) were added to the endothelial cell growth media the HUVECs actively proliferated *in vitro* for 7 days on the composite and hydrogel scaffolds at a

faster rate than on the textile scaffold. Compared to Day 1, the number of HUVECs at Day 7 had increased 2.69 ± 0.37 fold on the composite scaffold, 2.12 ± 0.08 fold on the hydrogel matrix, but only 1.41± 0.54 fold on the textile sample (composite vs. textile: p=0.003; hydrogel vs. textile: p=0.0428; composite vs. hydrogel: p=0.1147).

In summary, we found that the textile structure alone lacked the bioactivity to support HUVEC growth. The combination of textile and hydrogel materials significantly improved the viability and proliferation of the HUVECs attached to the scaffold during 7 days of cell culture.

3.5 The composite vascular graft showed macrophage cytocompatibility

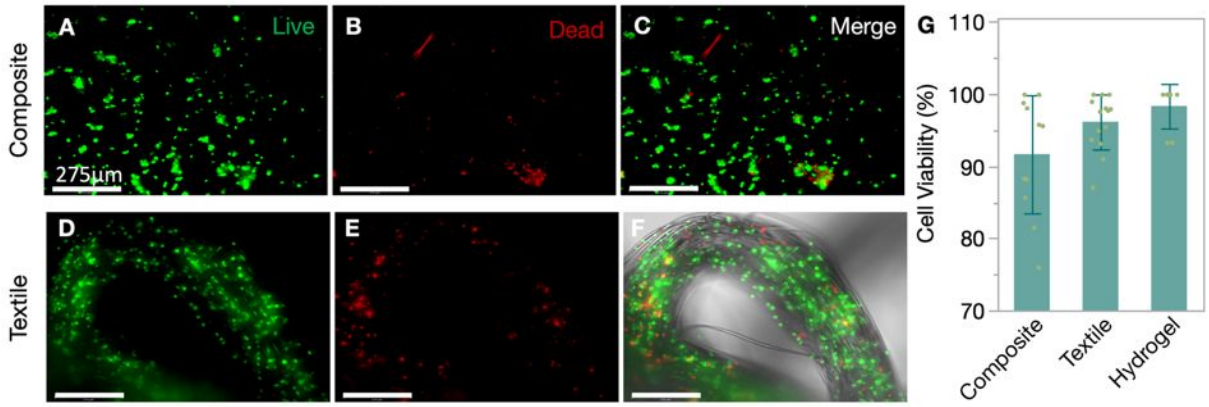

Figure 4. THP-1-derived macrophages cultured *in* vitro for 3 days on the composite textile/ hydrogel scaffold (A-C), and on the textile scaffold (D-F). Scale bar = 275 μm. (G) Macrophage viability on composite, textile, and hydrogel scaffolds.

In this study, we used THP-1 cell derived macrophages to study and compare their *in vitro* responses to the composite scaffold and the two separate components: the textile sample and hydrogel matrix. Macrophages retained a relatively high viability on all the components of the composite vascular graft (**Figure 4G**). There was no significant difference in the macrophage viability on the composite, textile and hydrogel scaffolds, indicating that both components of the composite vascular graft had good cytocompatibility to THP-1 cell-derived macrophages.

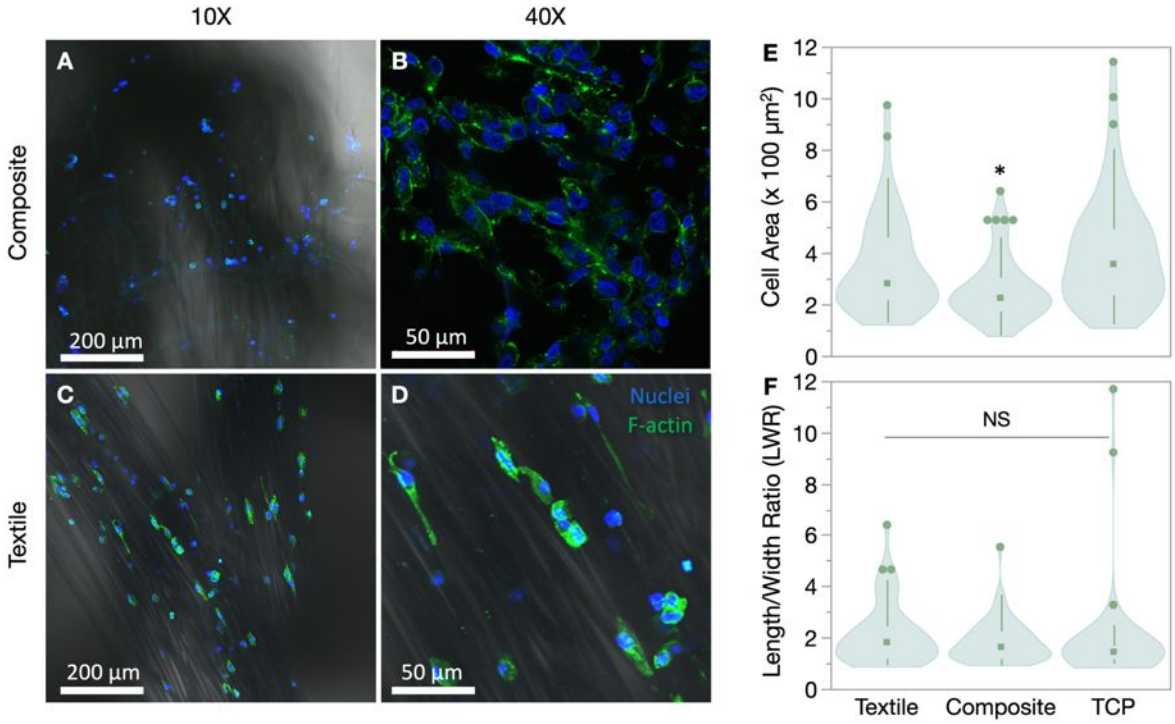

Figure 5. Confocal microscopies the THP-1-derived macrophages after *in vitro* culture for 7 days on the textile/hydrogel composite scaffold and on the PLA textile sample. Immunofluorescence staining of F-actin (green) and nuclei (blue) of the macrophages on the composite scaffold (A-B) and on the PLA textile scaffold (C-D). Scale bars: (A & C) 200 µm, (B & D) 50 µm. (E) Single cell area (E) and length/width ratio (F) of the cell was not changed significantly between the PLA textile sample, the composite scaffold, and the tissue culture plate (TCP) control. Triplicate images were recorded for each specimen and at least 30 measurements were conducted on each sample. *$p<0.05$. NS = no significant difference.

The cytoskeleton of the macrophages was stained by phalloidin on both the composite scaffolds and textile sample (**Figure 5**). There was a mixture of spindle-shape macrophages and spherical macrophages on both the composite scaffold (**Figure 5A-5B**) as well as on the textile sample (**Figure 5C-5D**). The distributions of the cell area (**Figure 5E**) and the cell length/width ratio (LWR) (**Figure 5F**) were asymmetric and skewed to the right, suggesting there was a larger population of small and round cells than large and elongated cells. The median cell area and LWR were reported and compared (**Figures 5E and 5F)**. Based on the non-parametric Steel-Dwass test for multiple comparisons, the median macrophage cell area on the composite scaffold was significantly smaller than that on the textile sample ($p=0.019$) or on the TCP control ($p<0.01$). But there was no statistical difference between the macrophage LWRs on the

composite, textile and TCP surfaces. Most cells exhibited a LWR close to 1, indicating a spherical cell morphology.

3.6 The composite vascular graft enhanced the expression of both M1 and M2 related genes in macrophages.

The gene expression of THP-1-cell-derived macrophages were monitored while cultured on the various scaffold materials. Compared to the TCP control, the presence of the biomaterial elicted the macrophage activation at a significantly higher level after 7 days of *in vitro* culture. This was confirmed by the elevated expression of both M1 and M2 related genes as shown in **Figure 6**. M1 genes were expressed at a higher level compared to M2 genes in general.

The M1 related genes, interferon regulatory factor 5 (IRF5), tumor necrosis factor-α (TNF-α), and interleukin-1β (IL-1β), were measured in this study. IRF5 is the transcription factor that drives the M1 phenotype in macrophages and correlates to atherosclerosis plaque vulnerability [26, 27]. It was only slightly upregulated by 1.5-fold by the composite graft when compared to the TCP control (**Figure 6A**). TNF-α was highly expressed in the lipopolysaccharide (LPS) activated M1 macrophages, which is 47-fold greater than inactivated monocytes and 4-fold greater than the TCP control (**Figure S5 A&B**). In response to the composite scaffold, TNF-α expression in macrophage was upregulated 6-fold compared to the TCP control (**Figure 6B**). Another M1 gene, IL-1, was upregulated 6.6-fold compared to the TCP control (**Figure 6C**).

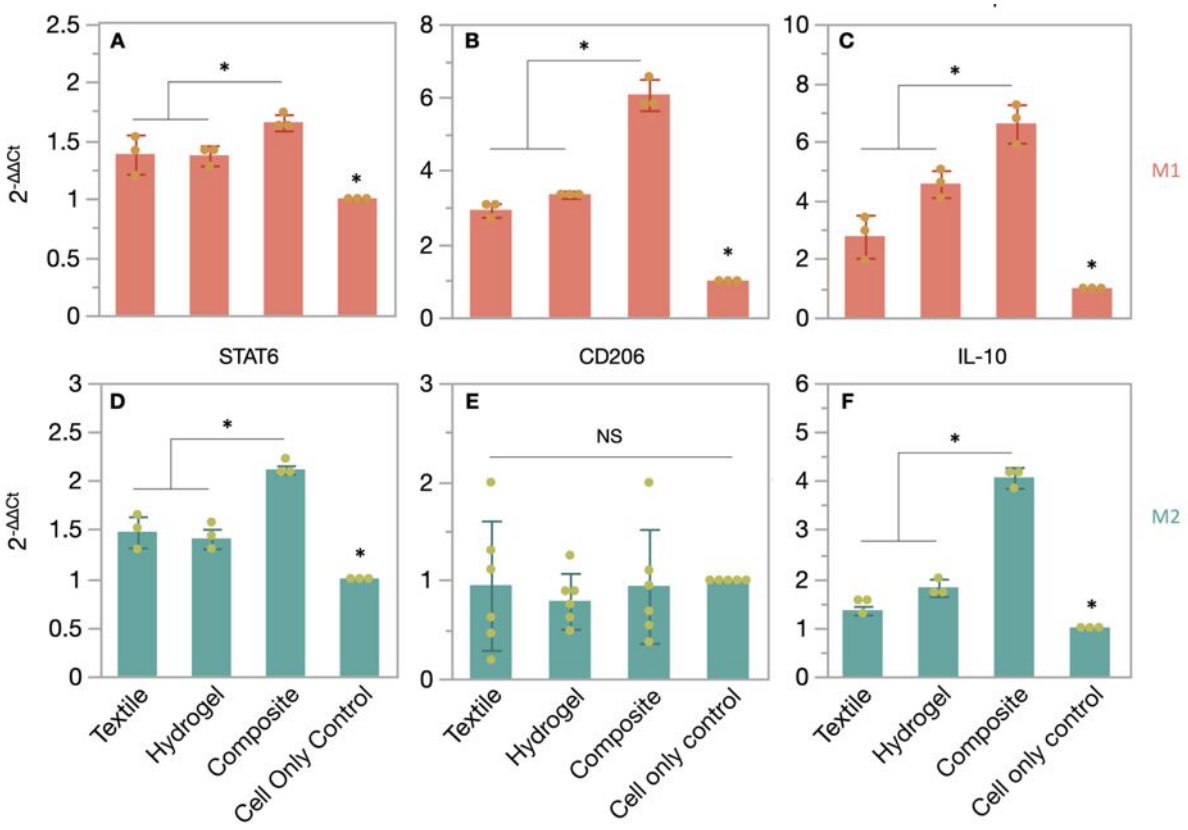

Figure 6. Gene expression of THP-1-derived macrophages following 7 days of *in vitro* culture on the PLA textile sample, GelMA hydrogel matrix, the textile/hydrogel composite and tissue culture plate (cell only) control. M1 macrophage related genes: (A) IRF5, (B) TNF-α, (C) IL-1β; M2 macrophage related genes: (D) STAT6, (E) CD206, (F) IL-10. *$p<0.05$, NS: non-significant. $n\geq3$.

The M2-related genes, signal transducer and activator of transcription 6 (STAT6) and interleukin 10 (IL-10), were also upregulated in macrophages by the composite graft, while mannose receptor C type 1 (MRC1 or CD206) remained unchanged.

STAT6 is a M2 transcription factor that drives the M2 phenotype as observed by the upregulation of M2-related genes such as arginase 1 (Arg1) and CD206 [33,34]. In this study it was upregulated in macrophages 2-fold by the composite scaffold and merely 1.5-fold by the textile and hydrogel matrix samples (**Figure 6D**). CD206 was highly expressed in IL-4 induced M2 macrophages, 3-fold times greater than non-adherent monocytes and 21-fold times more than adherent macrophages on the TCP control (**Figure S5 C&D**). However, no significant

difference was observed in the expression of CD206 in macrophages on the composite scaffold compared to the TCP control (**Figure 6E**). IL-10 was upregulated 4 fold by the composite scaffold, 1.3 fold by the textile sample, and 1.8 fold by the hydrogel matrix (**Figure 6F**).

3.7 The composite vascular graft upregulated genes related to the vascularization and tissue remodeling.

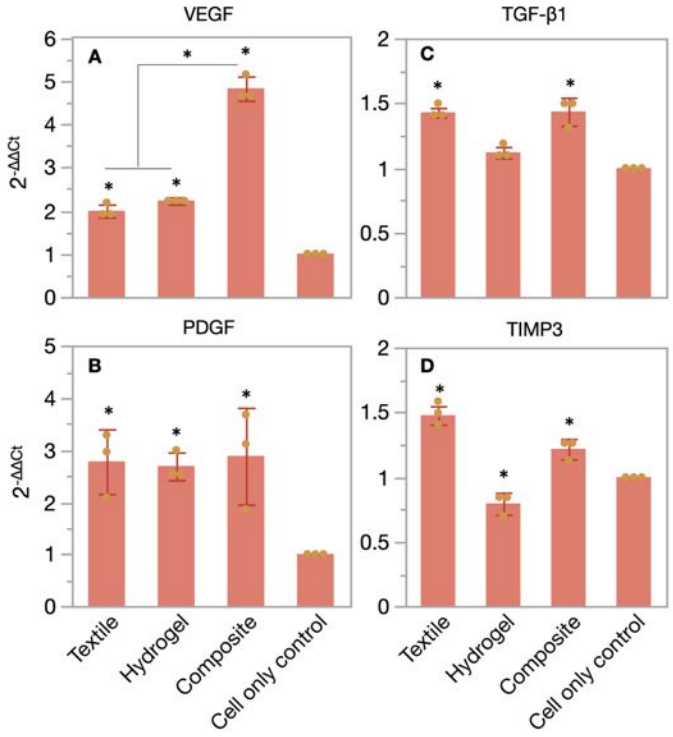

Figure 7. Vascularization-related gene expression of THP-1-derived macrophages after culturing for 7 days) *in vitro* on textile, hydrogel, textile/hydrogel composite and tissue culture plate (TCP) control samples: (A) VEGF, (B) PDGF, (C) TGF-β1, (D) TIMP-3. *p<0.05, n=3.

After studying the gene expression related to macrophage activation and phenotype, we further looked at the macrophage gene expression related to vascular tissue regeneration and vascular graft remodeling. Vascular endothelial growth factor (VEGF) was significantly upregulated in macrophages cultured on the textile and hydrogel scaffolds compared to the tissue culture plate (TCP) control (**Figure 7A**). The combination of the textile and hydrogel further increased VEGF gene expression compared to the scaffolds with only textile and hydrogel components (4.82 versus 1.99 and 2.23, p<0.0001). The macrophage platelet-derived growth factor (PDGF)

was also significantly upregulated by the composite (2.89, $p<0.05$), textile (2.78, $p<0.05$) and hydrogel samples (2.69, $p<0.05$) compared to the TCP control (**Figure 7B**).

Transforming growth factor-beta 1 (TGF-β1) is another important factor that mediates vascular graft stenosis and remodeling [37]. TGF-β1 expression remained unchanged on all three samples compared to the TCP control (**Figure 7C**).

The tissue inhibitor matrix metalloprotease-3 (TIMP-3) also participates in vascular graft remodeling. In this study, the material did not elicit changes in the expression of TIMP-3. The textile scaffold elicited only 1.47-fold higher TIMP-3 gene expression than the TCP control, which might be due to the extensive exposure of synthetic PLA polymer to macrophages. On the other hand, the hydrogel scaffold downregulated TIMP-3 gene expression to 0.79-fold compared to the TCP control. Synergistically, the TIMP-3 gene expression in macrophages on the composite scaffold was similar to the TCP control (1.21 versus 1, $p=0.018$) (**Figure 7D**), which might be explained by the hydrogel encapsulating the textile component and reducing the contact between the macrophages and the PLA textile material.

3.8 Endothelial cell migration was enhanced by the macrophage conditioned media cultured on the composite vascular graft

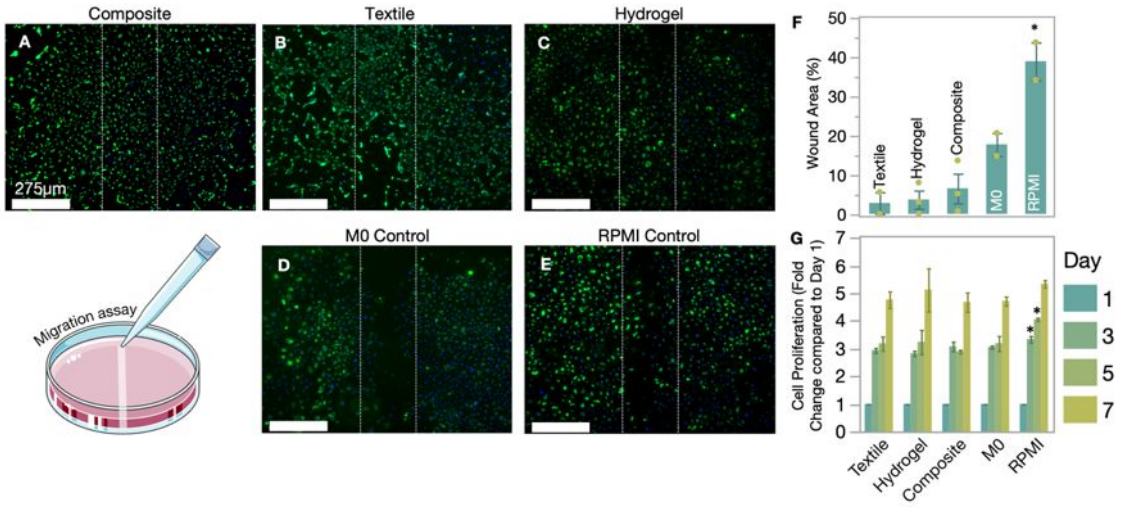

Figure 8. Macrophage conditioned media (CM) accelerated EC migration in a scratch assay. The CM collected from macrophages cultured on (A) the textile/hydrogel composite scaffold,

(B) the textile scaffold, (C) the hydrogel scaffold. Two controls were included: (D) CM from M0 macrophages was added to ECs to study the effect of macrophage CM on ECs; (E) RPMI basal media mixed with complete EC media at a ratio of 1:1 was also used as a media control. Scale bar = 275 μm. White dash lines on the images indicate the original scratch across the EC monolayer. (F) Effect of macrophage CM on EC scratch area. (G) Macrophage CM showed no significant impact on EC proliferation over 7 days. *$p<0.05$. NS: no statistical significance. The cell migration assay illustration was created using templates from Servier Medical Art under the Creative Commons Attribution 3.0 Unported License.

As mentioned previously, critical to the success of a vascular graft is the rapid formation of a continuous, intact and functional endothelium on the luminal surface. After seeing the upregulation of the angiogenic genes, VEGF and PDGF, in macrophages cultured on the composite scaffold, further investigations were pursued to determine if macrophages could increase EC migration and proliferation in a paracrine manner. Macrophages were cultured on composite, textile, hydrogel and TCP scaffolds, and the supernatant conditioned media (CM) was collected every other day and used to treat the EC monolayer on a TCP.

A scratch assay was used to study EC migration when cultured in macrophage CM (**Figure 8**). A scratch was created on a single-layer of ECs cultured on TCP (**Figure 8A-8E**). Macrophage CM was added to theECs for 24 h and the migration of the ECs across the scratch wound was measured. It was found that macrophage CM was able to accelerate EC migration within 24 hours as indicated by a smaller wound area compared to the media only control which contain fresh 1:1 RPMI:EC complete medium (**Figure 8F**). In particular, macrophages cultured on the three scaffold materials, that is the composite, textile and hydrogel samples were able to further increase the cell migration rate compared to the macrophages cultured on a tissue culture plate. This might be explained to the enhanced macrophage activation and the upregulation of genes such as VEGF in macrophages on the scaffold materials (**Figure 6** and **7**).

Using the alamarBlue® assay, EC proliferation was also quantified during culture in macrophage CM over 7 days. Although the macrophage CM was able to promote EC migration,

it did not promote the EC proliferation compared to the fresh media control. In fact it even slowed down the EC proliferation during the initial 5 days (**Figure 8G**).

4. Discussion

Tissue-engineered vascular grafts fabricated from synthetic polymers usually lack a positive cellular response and can potentially retard the regeneration process. Natural polymers have long been considered as viable materials to promote tissue regeneration and revascularization, but their use has been limited by their inferior mechanical properties. In this study, a composite vascular graft was successfully engineered using a knitted poly(lactic acid) textile reinforcement and a gelatin methacryloyl hydrogel matrix. The textile reinforcement provided satisfactory mechanical performance, and at the same time, the hydrogel matrix promoted endothelial cell survival, adhesion, and proliferation. The combination of the textile and the hydrogel components also enhanced M1 and M2 macrophage gene expression and upregulated angiogenic genes such as VEGF and PDGF, which further encouraged endothelial cell migration. In addition to its role in promoting positive cellular response, the hydrogel also sealed the large pores of the textile structure and eliminated fluid leakage through the graft wall under pressure. This in turn will positively regulate hemodynamic flow and fabricate a more clinically secure and successful vascular graft.

Compliance is one of the most critical mechanical properties needed by a vascular graft so as to achieve ultimate success in the clinic [18,42,43]. The mechanical mismatch at the anastomosis of a stiff vascular graft and a flexible host blood vessel can elevate the intraluminal stress at the anastomosis and cause the suture-line intimal hyperplasia [44]. In this study, we found that the initial radial compliance of the composite vascular graft was comparable to the compliance of the human saphenous vein, the current gold standard, which suggests that the compliance of the composite vascular graft is acceptable for this type of application. It is worth noting that the compliance of the composite vascular graft was higher than the textile scaffold

alone. This may be due to the coating of the elastic hydrogel matrix that was added to improve the hemostasis of the vascular graft [45].

The strength of the vascular graft determines the safety of the vascular graft once implanted. As shown in this study, the PLA textile reinforcement provided the primary mechanical strength, but there are many factors that can influence the bursting strength and suture retention strength of a vascular graft, including, but not limited to, the type of material [46], the structural design [47,48,49], the density and thickness [50,51], the method of fabrication [52] and post-fabrication treatments such as crosslinking and heat-setting [6,13,53]. We particularly investigated the impact of the number of PLA filaments that were plied together for the fabrication of the textile reinforcement. Incorporating more ends of PLA filaments increased the thickness and strength of the multifilament yarn [6]. It also caused the final knitted structure to have a smaller average pore size, a tighter structure, a stronger bursting strength but a lower radial compliance. The 2-ply PLA conduit was selected for the textile reinforcement due to its stable structure and acceptable mechanical performance.

Like any implantable biomaterial, the basic requirement for the composite vascular graft is cytocompatibility, which means that the material is not toxic to cells and does not induce cell death. In this study, we cultured two types of cells, macrophages and endothelial cells, on the three types of materials so as to evaluate their cytocompatibility. Both cell types are important components of a regenerated vascular graft and showed high viability on our graft materials.

The luminal surface of a healthy blood vessel is lined by a continuous single layer of endothelial cells, which contacts the blood directly, playing a critical role in regulating hemostasis [23]. Successful and rapid endothelization on the luminal surface of a vascular graft will terminate the coagulation cascade and prevent stenosis and occlusion of the blood vessel [57]. The reendothelization on the luminal surface of a vascular graft is of great importance for its success.

In this study the combination of the textile and hydrogel components presented good cytocompatibility to endothelial cells. Although endothelial cells had a lower viability on the synthetic textile scaffold, the introduction of the hydrogel was able to significantly increase the endothelial cell viability. The study also demonstrated that the number of endothelial cells attached and proliferated on the composite scaffold improved due to the addition of the hydrogel component. Such properties of the composite vascular graft might promote a rapid re-endothelization *in vivo*.

Macrophages are the innate immune cells that are among the first responders to a foreign implant. They are among the key mediators that signal vascular tissue cell activity and determine the vascular graft's process of regeneration or restenosis [40,54]. Early studies on vascular grafts attempted to circumvent the activation of the immune system to prevent hyperplasia and adverse remodeling. However, the immune response is inevitable after implanting a foreign material. Immune cells are rapidly recruited to the biomaterial after implantation and actively regulate the subsequent tissue regeneration process by setting up an immune microenvironment [55]. Moreover, eliminating or avoiding macrophage activation does not benefit the situation, but instead prevents the tissue regeneration process [25]. M1 macrophages are pro-inflammatory. They predominate the cell population at the early stage following implantation and express proinflammatory cytokines such as TNF-α and IL-1β. M1 macrophages also release a high level of angiogenic cytokines such as VEGF. They are able to promote endothelial cell migration and proliferation, which is beneficial to the endothelization of the vascular graft. However, their prolonged presence can prevent vascular maturation, decrease endothelial cell proliferation, and induce vascular graft stenosis [17]. M2 is an anti-inflammatory and pro-regenerative phenotype. They consist of subtypes that assume distinct functions. For example, the M2a subtype can be induced by IL-4 and IL-13 and the M2c subtype

can be induced by IL-10 [25]. They release high levels of PDGF that can stabilize the vascular cells and regulate deposition of extracellular matrix and graft remodeling [68].

In this study, macrophages showed a high viability and did not show differences between the textile and hydrogel components of the composite vascular graft. After 7 days of *in vitro* culture, the composite vascular graft enhanced the activation of macrophages, evidenced by upregulating both M1-related genes, TNF-α and IL-1β, and M2-related genes, STAT6 and IL-10, but not IRF5 and CD206.

TNF-α is known to promote the differentiation of endothelial progenitor cells [28] and induce the secretion of IL-8 to promote phagocyte recruitment and their adhesion to the endothelium. IL-1β has been identified as a treatment target for atherosclerosis, given that its presence promotes coagulation, leukocyte-to-EC adhesion, and SMC proliferation [29, 30]. Blockage of IL-1β has been observed to reduce SMC proliferation which is thought to reduce the risk of intimal hyperplasia in vascular grafts [29]. However, IL-1β was also reported to mediate vascular endothelial growth factor (VEGF) and induce the production of nitric oxide from ECs, which is known to benefit the endothelization process of vascular grafts [31, 32]. Therefore, the upregulation of TNF-α and IL-1β by the composite graft could potentially reduce the risk of graft stenosis and promote endothelization.

On the other hand, M2 genes STAT6 and IL10 were also upregulated. Upregulation of STAT6 has been reported to enhance the efferocytosis in macrophages to remove apoptotic cell debris and resolve inflammation [35]. The expression and phosphorylation of STAT6 was also found to decrease in the unstable and vulnerable atherosclerotic plaque in mice [33], and marginal upregulation of STAT6 by the composite material after 7 days of *in vitro* cell culture might mitigate the subsequent implant-induced inflammation around a vascular graft in the case of *in vivo* implantation. IL-10 is known to reduce inflammation, increase the survival and migration

of human endothelial progenitor cells (EPC), and upregulate VEGF expression in a murine myocardial infarction (MI) model [36]. The significant upregulation of IL-10 by the composite vascular graft can potentially benefit the regeneration of the TEVG *in situ*.

Such a hybrid gene expression profile of M1- and M2-related genes might suggest a mixture of M1 and M2 macrophages or a transition from M1 to M2 macrophages. O'Brien et al demonstrated that previously activated M1 macrophages were readily primed to an M2-like phenotype (M1-M2), which showed enhanced angiogenic gene expression, compared to M2 macrophages derived from inactivated M0 macrophages (M0-M2) [58]. These M1-M2 macrophages were able to accelerate endothelial cell migration compared to the M0-M2 macrophages [58].

In this study, the composite scaffold also showed a significantly higher level of macrophage gene expression in TNF-α, IL-1β, IL-10 and VEGF, compared to the textile and hydrogel scaffolds, which may have been the synergistic effect of its two components. The heterogenicity of the composite material may also have contributed to the higher level of macrophage activation. Li et al showed a similar *in vivo* result from his fiber-hydrogel composite scaffold made from a poly(ε-caprolactone) (PCL) textile and a hyaluronic acid (HA) hydrogel matrix. His scaffold recruited more $CD68^+$ (pan macrophages), $CD86^+$ (M1), $CD206^+$ (M2) and $CD86^+CD206^+$ macrophages compared to the 100% HA hydrogel control [59].

Similar to O'Brien et al's results, we found that the macrophages cultured on the composite graft showed upregulated angiogenic gene expression of VEGF and PDGF. This result also agrees with Li et al that a fiber-hydrogel composite was more pro-angiogenic than the hydrogel alone scaffold [59]. VEGF has been reported to be highly involved throughout the vascular graft remodeling process [60] and plays a critical role in maintaining graft patency [61]. Upregulated VEGF may also further enhance monocyte recruitment and contribute to

endothelium formation within the vascular graft. As previously reported by Smith et al, circulating monocytes expressing VEGF receptors can be recruited to the VEGF-immobilized vascular graft surface and contribute to the newly formed endothelium which co-expresses the macrophage and endothelial cell markers [62]. Myeloid cell-derived PDGF-B is critical to macrophage survival, reducing neotissue formation and slowing down polymer degradation of the vascular graft scaffold [37]. M2a macrophages have been reported to release a high level of PDGF-BB that stabilizes pericytes and promotes the migration and differentiation of vascular SMCs and pericytes [24].

The expression of TGF-β1 and TIMP-3 were not found to change in macrophages on the composite scaffold compared to the TCP control. Both genes are highly involved in the vascular remodeling process. TGF-β1 can promote EC migration and vessel formation and is highly involved in endothelial-mesenchymal cell crosstalk to stabilize blood vessels [25]. It also promotes SMC migration, proliferation and ECM production [38]. However, the uncontrolled and extensive proliferation of vascular tissue cells may not be beneficial as they can cause anastomotic intimal hyperplasia and graft stenosis. Inhibiting TGF-β1 was found to reduce hyperplasia and graft stenosis by mitigating M1 macrophage activation and mesenchymal cell expansion [39]. While the upregulation of TGF-β1 at an early-stage post implantation is likely to facilitate the influx of ECs and SMCs, a longer-term presence may lead to excessive proliferation, hyperplasia and stenosis of the graft. TIMP-3 is highly expressed in M2a macrophages; it inhibits matrix metallopeptidase 9 (MMP9) and reduces angiogenic activity [40]. Its overexpression has been reported to elicit apoptosis of isolated vascular SMCs and to significantly reduce neointima formation in a vein graft [41].

The conditioned media of the macrophages cultured on the composite vascular graft also promoted EC migration *in vitro*. Graney et al demonstrated that M1 macrophages enriched the gene expression of tip cells and EC migration [24]. O'Brien et al found that M1-derived M2

macrophages were able to promote EC migration compared to M0-derived M2 macrophages [58], while Spiller et al found that macrophages in their M0, M1 and M2c phenotypes were able to increase EC sprouting in Matrigel *in vitro* [40]. M1 macrophages triggered EC tip cell sprouting via VEGF, TNF-α and IL-1β. M2 macrophages, on the other hand, were observed to promote EC anastomosis under an unidentified mechanism [40]. Scaffolds carrying M1-inducing interferon-γ (IFN-γ) enhanced *in vivo* vascular infiltration compared to those carrying M2a-inducing interleukin-4 (IL-4) and the bare scaffold control [56].

Interestingly, although there is evidence of macrophages promoting vascularization in the literature [25, 40, 56], in this study, we found that the biomaterial-activated macrophages were only able to promote EC migration but not EC proliferation *in vitro*. Similarly, O'Brien et al also found that macrophages, regardless of their phenotype, do not promote EC proliferation *in vitro* [58]. Graney et al also found that different macrophage phenotypes are not associated with different EC proliferation marker expression *in vitro* [24].

Because of the limitations in this study we recommend further work to address these issues. With the two-dimensional cell culture model in this study, we were able to demonstrate basic cellular activities such as endothelial cell viability, migration and proliferation and macrophage polarization [63,64,65]. However, the lack of a complete immune system and dynamic blood flow makes it hard to completely simulate *in vivo* events. Therefore, a thorough *in vivo* study in a clinical-relevant animal model will be important in order to validate the post-implantation performance of the graft and to study the synergistic effects of immune system and tissue cells in the regenerative process.

In addition, optimizing the design of the hydrogel matrix, such as modifying the formulation, pore size and stiffness, could further tune the macrophage response. Encapsulating immunomodulatory cytokines in the hydrogel matrix could potentially alter the macrophage

phenotype toward promoting vascular regeneration [28,62,66,67,68]. Optimizing the pore size and stiffness of the hydrogel matrix for macrophage response and vascular regeneration could also be important. Garg et al previously indicated that the pore size of an electrospun polydioxanone mesh could alter macrophage gene expression [69]. A larger pore size caused by thicker fibers in an electrospun scaffold could upregulate M2-related genes while smaller pores and thinner fibers could upregulate M1-related genes [69]. A similar impact has also been shown when using a GelMA hydrogel [70]. The pore size of the material could further affect the vascular regeneration and remodeling process. Tara et al concluded that the larger pore size of their vascular graft was associated with fewer macrophages after 12-month implantation in mice accompanied by a lower level of graft calcification [71]. With that said, we suggest further work is needed to engineer the hydrogel matrix so as to optimize the graft's performance.

Overall, the textile/hydrogel composite vascular graft reported in this study showed satisfactory mechanical properties and encouraging cell responses *in vitro*, making it a promising candidate for further evaluation in a clinically relevant animal model.

5. Conclusions

In the current study, we have successfully designed and fabricated a composite vascular graft by combining textile fibers with a hydrogel matrix. The textile reinforcement was knitted into a seamless conduit using a biodegradable poly(lactic acid) multifilament yarn, which provided excellent mechanical reinforcement which exceeded the requirement for a vascular graft. The hydrogel matrix, made from gelatin methacryloyl hydrogel, provided a surface that promoted endothelial cell survival, adhesion and proliferation. The combination of the textile and hydrogel components enhanced the macrophage activation by generating both M1 pro-inflammatory and M2 pro-regenerative phenotypes which upregulated the vascularization-related genes such as VEGF and PDGF after 7 days of *in vitro* cell culture. The conditioned media collected from activated macrophages by the composite graft were able to accelerate

endothelial cell migration *in vitro*, which is expected to facilitate a more rapid endothelization on the luminal surface of the composite vascular graft. Overall, the textile-reinforced composite vascular graft described in this study showed promising *in vitro* results toward the successful *in situ* endothelization and therefore is recommended for further evaluation in a clinically relevant animal model.

Acknowledgements:

This work was supported by the North Carolina Textile Foundation (MWK), and American Association of Textile Chemists and Colorists Student Research Support Grant (FZ) and National Science Foundation (DBI-1624613) (NC State Cellular and Molecular Imaging Facility). Special thanks to our colleagues at NC State University for their assistance, particularly: Eric Lawrence at The Nonwoven Institute's Fiber Science Lab for training on the Lamb circular knitting machine for fabricating the textile conduits, Hai Bui at the Wilson College of Textiles for fabricating the Teflon mold, Judy Elson at the Wilson College of Textiles for collecting the scanning electron microscope images, Dr. Jesse Jur for providing the MTS mechanical tester, Dr. Mariusz Zareba and Dr. Eva Johannes at the Cellular and Molecular Imaging Facility for the training on the Zeiss LSM 880 confocal microscope, Dr. Xiaoyan Sun at the Molecular Education, Technology and Research Innovation Center for undertaking the nuclear magnetic resonance measurements, Dr. Susan Bernacki and Dr. Douglas Tremblay in the Joint Department of Biomedical Engineering for the development of the histological protocol and undertaking the ethylene oxide sterilization procedure. This research would not have been accomplished without their valuable contribution.

A textile-reinforced hydrogel was designed and fabricated into a scaffold to generate a tissue-engineered vascular graft. The textile reinforcement provided the mechanical robustness to satisfy the mechanical requirements while the hydrogel matrix significantly improved endothelial cell adhesion and proliferation *in vitro*. The composite vascular graft also enhanced macrophage activation by upregulating M1 and M2 genes, which further increased endothelial cell migration *in vitro*.

References:

1. Matsuzaki Y, John K, Shoji T, Shinoka T. The evolution of tissue engineered vascular graft technologies: from preclinical trials to advancing patient care. Applied Sciences 2019;9:1274.
2. Pashneh-Tala S, MacNeil S, Claeyssens F. The tissue-engineered vascular graft—past, present, and future. Tissue Engineering Part B: Reviews 2016;22:68-100.
3. King MW, Bambharoliya T, Ramakrishna H, Zhang F. Definitions and basic mechanism of coronary artery disease (CAD). In: King MW, editor. Coronary Artery Disease and The Evolution of Angioplasty Devices: Springer, 2020. p. 3-10.
4. Hibino N, McGillicuddy E, Matsumura G, Ichihara Y, Naito Y, Breuer C, et al. Late-term results of tissue-engineered vascular grafts in humans. J Thorac Cardiovasc Surg 2010;139:431-436. e2.
5. King MW, Chen J, Deshpande M, He T, Ramakrishna H, Xie Y, et al. Structural Design, Fabrication and Evaluation of Resorbable Fiber-Based Tissue Engineering Scaffolds. Biotechnol Bioeng 2019:61-188.
6. Zhang F, Bambharoliya T, Xie Y, Liu L, Celik H, Wang L, et al. A hybrid vascular graft harnessing the superior mechanical properties of synthetic fibers and the biological performance of collagen filaments. Materials Science and Engineering: C 2021;118:111418.
7. Reinhardt JW, Rosado, Juan de Dios Ruiz, Barker JC, Lee Y, Best CA, Yi T, et al. Early natural history of neotissue formation in tissue-engineered vascular grafts in a murine model. Regenerative Medicine 2019;14:389-408.
8. Cha B, Shin SR, Leijten J, Li Y, Singh S, Liu JC, et al. Integrin-mediated interactions control macrophage polarization in 3D hydrogels. Advanced Healthcare Materials 2017;6:1700289.
9. Loessner D, Meinert C, Kaemmerer E, Martine LC, Yue K, Levett PA, et al. Functionalization, preparation and use of cell-laden gelatin methacryloyl–based hydrogels as modular tissue culture platforms. Nature Protocols 2016;11:727-746.
10. Zhang F, King MW. Biodegradable polymers as the pivotal player in the design of tissue engineering scaffolds. Advanced Healthcare Materials 2020;9:1901358.
11. Margerrison E, Argentieri M, Schoelles K, Lucas S. Medical Device Material Performance Study - Poly Lactic-co-Glycolic Acid [P(L/G)A] Safety Profile. U.S. FDA Center for Devices and Radiological Health; Emergency Care Research Institute 2020.
12. Xie Y, Zhang F, Akkus O, King MW. A collagen/PLA hybrid scaffold supports tendon-derived cell growth for tendon repair and regeneration. Journal of Biomedical Materials Research Part B: Applied Biomaterials 2022.
13. Zhang F, Xie Y, Celik H, Akkus O, Bernacki SH, King MW. Engineering small-caliber vascular grafts from collagen filaments and nanofibers with comparable mechanical properties to native vessels. Biofabrication 2019;11:035020.

14. Annabi N, Nichol JW, Zhong X, Ji C, Koshy S, Khademhosseini A, et al. Controlling the porosity and microarchitecture of hydrogels for tissue engineering. Tissue Engineering Part B: Reviews 2010;16:371-383.
15. Liu J, Chen D, Zhu X, Liu N, Zhang H, Tang R, Liu Z. Development of a decellularized human amniotic membrane-based electrospun vascular graft capable of rapid remodeling for small-diameter vascular applications. Acta Biomaterialia. 2022;152:144-56.
16. Chen L, Li Z, Zheng Y, Zhou F, Zhao J, Zhai Q, Zhang Z, Liu T, Chen Y, Qi S. 3D-printed dermis-specific extracellular matrix mitigates scar contraction via inducing early angiogenesis and macrophage M2 polarization. Bioactive materials. 2022 Apr 1;10:236-46.
17. Tang D, Chen S, Hou D, Gao J, Jiang L, Shi J, Liang Q, Kong D, Wang S. Regulation of macrophage polarization and promotion of endothelialization by NO generating and PEG-YIGSR modified vascular graft. Materials Science and Engineering: C. 2018 Mar 1;84:1-1.
18. Salacinski HJ, Goldner S, Giudiceandrea A, Hamilton G, Seifalian AM, Edwards A, et al. The mechanical behavior of vascular grafts: a review. J Biomater Appl 2001;15:241-278.
19. Yang X, Wang L, Guan G, King MW, Li Y, Peng L, et al. Preparation and evaluation of bicomponent and homogeneous polyester silk small diameter arterial prostheses. J Biomater Appl 2014;28:676-687.
20. ISO. ISO 7198: 2016
cardiovascular implants and extracorporeal systems - vascular prostheses - tubular vascular grafts and vascular patches. 2nd ed. : International Organization for Standardization., 2016.
21. Abbott WM, Megerman J, Hasson JE, L'Italien G, Warnock DF. Effect of compliance mismatch on vascular graft patency. Journal of vascular surgery 1987;5:376-382.
22. Maleckis K, Kamenskiy A, Lichter EZ, Oberley-Deegan R, Dzenis Y, MacTaggart J. Mechanically tuned vascular graft demonstrates rapid endothelialization and integration into the porcine iliac artery wall. Acta Biomaterialia 2021;125:126-137.
23. Radke D, Jia W, Sharma D, Fena K, Wang G, Goldman J, et al. Tissue engineering at the blood-contacting surface: A review of challenges and strategies in vascular graft development. Advanced healthcare materials 2018;7:1701461.
24. Li P, Li Y, Li Z, Wu Y, Zhang C, Wang C, et al. Cross talk between vascular smooth muscle cells and monocytes through interleukin-1β/interleukin-18 signaling promotes vein graft thickening. Arterioscler Thromb Vasc Biol 2014;34:2001-2011.
25. Graney PL, Ben-Shaul S, Landau S, Bajpai A, Singh B, Eager J, et al. Macrophages of diverse phenotypes drive vascularization of engineered tissues. Science Advances 2020;6:eaay6391.
26. Edsfeldt A, Swart M, Singh P, Dib L, Sun J, Cole JE, et al. Interferon regulatory factor-5-dependent CD11c macrophages contribute to the formation of rupture–prone atherosclerotic plaques. Eur Heart J 2022.
27. Leipner J, Dederichs T, von Ehr A, Rauterberg S, Ehlert C, Merz J, et al. Myeloid cell-specific Irf5 deficiency stabilizes atherosclerotic plaques in Apoe–/–mice. Molecular metabolism 2021;53:101250.
28. Wong MM, Chen Y, Margariti A, Winkler B, Campagnolo P, Potter C, et al. Macrophages control vascular stem/progenitor cell plasticity through tumor necrosis factor-α–mediated nuclear factor-κB activation. Arterioscler Thromb Vasc Biol 2014;34:635-643.
29. Libby P. Interleukin-1 beta as a target for atherosclerosis therapy: biological basis of CANTOS and beyond. J Am Coll Cardiol 2017;70:2278-2289.

30. Ridker PM, Everett BM, Thuren T, MacFadyen JG, Chang WH, Ballantyne C, et al. Antiinflammatory therapy with canakinumab for atherosclerotic disease. N Engl J Med 2017;377:1119-1131.
31. Kanno K, Hirata Y, Imai T, Iwashina M, Marumo F. Regulation of inducible nitric oxide synthase gene by interleukin-1 beta in rat vascular endothelial cells. American Journal of Physiology-Heart and Circulatory Physiology 1994;267:H2318-H2324.
32. Fahey E, Doyle SL. IL-1 family cytokine regulation of vascular permeability and angiogenesis. Frontiers in Immunology 2019;10:1426.
33. Gong M, Zhuo X, Ma A. STAT6 upregulation promotes M2 macrophage polarization to suppress atherosclerosis. Medical science monitor basic research 2017;23:240.
34. Yu T, Gan S, Zhu Q, Dai D, Li N, Wang H, et al. Modulation of M2 macrophage polarization by the crosstalk between Stat6 and Trim24. Nature communications 2019;10:1-15.
35. Cai W, Dai X, Chen J, Zhao J, Xu M, Zhang L, et al. STAT6/Arg1 promotes microglia/macrophage efferocytosis and inflammation resolution in stroke mice. JCI insight 2019;4.
36. Krishnamurthy P, Thal M, Verma S, Hoxha E, Lambers E, Ramirez V, et al. Interleukin-10 deficiency impairs bone marrow–derived endothelial progenitor cell survival and function in ischemic myocardium. Circ Res 2011;109:1280-1289.
37. Bonito V, Smits A, Goor O, Ippel BD, Driessen-Mol A, Münker T, et al. Modulation of macrophage phenotype and protein secretion via heparin-IL-4 functionalized supramolecular elastomers. Acta biomaterialia 2018;71:247-260.
38. Liu Y, Rayatpisheh S, Chew SY, Chan-Park MB. Impact of Endothelial Cells on 3D Cultured Smooth Muscle Cells in a Biomimetic Hydrogel. ACS Applied Materials & Interfaces 2012;4:1378-1387.
39. Lee Y, Ruiz-Rosado JdD, Mahler N, Best CA, Tara S, Yi T, et al. TGF-β receptor 1 inhibition prevents stenosis of tissue-engineered vascular grafts by reducing host mononuclear phagocyte activation. The FASEB Journal 2016;30:2627-2636.
40. Spiller KL, Anfang RR, Spiller KJ, Ng J, Nakazawa KR, Daulton JW, et al. The role of macrophage phenotype in vascularization of tissue engineering scaffolds. Biomaterials 2014;35:4477-4488.
41. George SJ, Lloyd CT, Angelini GD, Newby AC, Baker AH. Inhibition of late vein graft neointima formation in human and porcine models by adenovirus-mediated overexpression of tissue inhibitor of metalloproteinase-3. Circulation 2000;101:296-304.
42. Zhalmuratova D, La TG, Yu KT, Szojka AR, Andrews SH, Adesida AB, Kim CI, Nobes DS, Freed DH, Chung HJ. Mimicking "J-Shaped" and Anisotropic Stress–Strain Behavior of Human and Porcine Aorta by Fabric-Reinforced Elastomer Composites. ACS applied materials & interfaces. 2019;11(36):33323-35.
43. Kuthe S, Schlothauer A, Bodkhe S, Hulme C, Ermanni P. 3D printed mechanically representative aortic model made of gelatin fiber reinforced silicone composite. Materials Letters. 2022 Aug 1;320:132396.
44. Ballyk PD, Walsh C, Butany J, Ojha M. Compliance mismatch may promote graft–artery intimal hyperplasia by altering suture-line stresses. J Biomech 1997;31:229-237.
45. Huang Y, King DR, Sun TL, Nonoyama T, Kurokawa T, Nakajima T, Gong JP. Energy-dissipative matrices enable synergistic toughening in fiber reinforced soft composites. Advanced functional materials. 2017;27(9):1605350.
46. Zia AW, Liu R, Wu X. Structural design and mechanical performance of composite vascular grafts. Bio-Design and Manufacturing. 2022 Aug 23:1-29.
47. Zhalmuratova D, Chung HJ. Reinforced gels and elastomers for biomedical and soft robotics applications. ACS Applied Polymer Materials. 2020 Feb 4;2(3):1073-91.

48. Bailly L, Toungara M, Orgéas L, Bertrand E, Deplano V, Geindreau C. In-plane mechanics of soft architectured fibre-reinforced silicone rubber membranes. Journal of the mechanical behavior of biomedical materials. 2014;40:339-53.
49. Pickering E, Paxton NC, Bo A, O'Connell B, King M, Woodruff MA. 3D printed tubular scaffolds with massively tailorable mechanical behavior. Advanced Engineering Materials. 2022 Nov 1:2200479.
50. Lin S, Cao C, Wang Q, Gonzalez M, Dolbow JE, Zhao X. Design of stiff, tough and stretchy hydrogel composites via nanoscale hybrid crosslinking and macroscale fiber reinforcement. Soft matter. 2014;10(38):7519-27.
51. Stahl A, Hao D, Barrera J, Henn D, Lin S, Moeinzadeh S, Kim S, Maloney W, Gurtner G, Wang A, Yang YP. A bioactive compliant vascular graft modulates macrophage polarization and maintains patency with robust vascular remodeling. Bioactive materials. 2023;19:167-78.
52. Akbari M, Tamayol A, Bagherifard S, Serex L, Mostafalu P, Faramarzi N, Mohammadi MH, Khademhosseini A. Textile technologies and tissue engineering: a path toward organ weaving. Advanced healthcare materials. 2016;5(7):751-66.
53. Xie Y, Guan Y, Kim S, King MW. The mechanical performance of weft-knitted/electrospun bilayer small diameter vascular prostheses. Journal of the mechanical behavior of biomedical materials 2016;61:410-418.
54. Hibino N, Yi T, Duncan DR, Rathore A, Dean E, Naito Y, et al. A critical role for macrophages in neovessel formation and the development of stenosis in tissue-engineered vascular grafts. The FASEB Journal 2011;25:4253-4263.
55. Hibino N, Mejias D, Pietris N, Dean E, Yi T, Best C, et al. The innate immune system contributes to tissue-engineered vascular graft performance. The FASEB Journal 2015;29:2431-2438.
56. Spiller KL, Nassiri S, Witherel CE, Anfang RR, Ng J, Nakazawa KR, et al. Sequential delivery of immunomodulatory cytokines to facilitate the M1-to-M2 transition of macrophages and enhance vascularization of bone scaffolds. Biomaterials 2015;37:194-207.
57. Wang D, Li LK, Dai T, Wang A, Li S. Adult stem cells in vascular remodeling. Theranostics 2018;8:815.
58. O'Brien EM, Spiller KL. Pro-inflammatory polarization primes Macrophages to transition into a distinct M2-like phenotype in response to IL-4. J Leukoc Biol 2021.
59. Li X, Cho B, Martin R, Seu M, Zhang C, Zhou Z, et al. Nanofiber-hydrogel composite–mediated angiogenesis for soft tissue reconstruction. Science translational medicine 2019;11:eaau6210.
60. Roh JD, Sawh-Martinez R, Brennan MP, Jay SM, Devine L, Rao DA, et al. Tissue-engineered vascular grafts transform into mature blood vessels via an inflammation-mediated process of vascular remodeling. Proceedings of the National Academy of Sciences 2010;107:4669-4674.
61. Koobatian MT, Row S, Smith Jr RJ, Koenigsknecht C, Andreadis ST, Swartz DD. Successful endothelialization and remodeling of a cell-free small-diameter arterial graft in a large animal model. Biomaterials 2016;76:344-358.
62. Smith RJ, Nasiri B, Kann J, Yergeau D, Bard JE, Swartz DD, et al. Endothelialization of arterial vascular grafts by circulating monocytes. Nature Communications 2020;11:1622.
63. Richter E, Ventz K, Harms M, Mostertz J, Hochgräfe F. Induction of macrophage function in human THP-1 cells is associated with rewiring of MAPK signaling and activation of MAP3K7 (TAK1) protein kinase. Frontiers in Cell and Developmental Biology 2016;4:21.

64. Caires HR, Barros da Silva P, Barbosa M, Almeida CR. A co-culture system with three different primary human cell populations reveals that biomaterials and MSC modulate macrophage-driven fibroblast recruitment. J Tissue Eng Regen Med 2018;12:e1433-e1440.
65. Sridharan R, Cavanagh B, Cameron AR, Kelly DJ, O'Brien FJ. Material stiffness influences the polarization state, function and migration mode of macrophages. Acta Biomaterialia 2019;89:47-59.
66. Ding H, Zhong M, Kim YJ, Pholpabu P, Balasubramanian A, Hui CM, et al. Biologically Derived Soft Conducting Hydrogels Using Heparin-Doped Polymer Networks. ACS Nano 2014;8:4348-4357.
67. Wheeler KC, Jena MK, Pradhan BS, Nayak N, Das S, Hsu CD, et al. VEGF may contribute to macrophage recruitment and M2 polarization in the decidua. PLoS One 2018;13:e0191040.
68. Zhang F, King MW. Immunomodulation Strategies for the Successful Regeneration of a Tissue-Engineered Vascular Graft. Advanced Healthcare Materials 2022:2200045.
69. Garg K, Pullen NA, Oskeritzian CA, Ryan JJ, Bowlin GL. Macrophage functional polarization (M1/M2) in response to varying fiber and pore dimensions of electrospun scaffolds. Biomaterials 2013;34:4439-4451.
70. Zhuang Z, Zhang Y, Sun S, Li Q, Chen K, An C, et al. Control of matrix stiffness using methacrylate–gelatin hydrogels for a macrophage-mediated inflammatory response. ACS Biomaterials Science & Engineering 2020;6:3091-3102.
71. Tara S, Kurobe H, Rocco KA, Maxfield MW, Best CA, Yi T, et al. Well-organized neointima of large-pore poly (L-lactic acid) vascular graft coated with poly (L-lactic-co-ε-caprolactone) prevents calcific deposition compared to small-pore electrospun poly (L-lactic acid) graft in a mouse aortic implantation model. Atherosclerosis 2014;237:684-691.